Light (anti)nuclei production in Pb-Pb collisions at √sNN= 5.02 TeV

(ALICE Collaboration) Acharya, S.; ...; Erhardt, Filip; ...; Gotovac, Sven; ...; Jerčić, Marko; ...; Karatović, David; ...; ...

Source / Izvornik: **Physical Review C, 2023, 107**

Journal article, Published version
Rad u časopisu, Objavljena verzija rada (izdavačev PDF)

https://doi.org/10.1103/PhysRevC.107.064904

Permanent link / Trajna poveznica: https://urn.nsk.hr/urn:nbn:hr:217:829898

Light (anti)nuclei production in Pb-Pb collisions at $\sqrt{s_{NN}} = 5.02$ TeV

S. Acharya *et al.**
(ALICE Collaboration)

(Received 10 February 2023; accepted 16 May 2023; published 8 June 2023)

The measurement of the production of deuterons, tritons and ^{3}He and their antiparticles in Pb-Pb collisions at $\sqrt{s_{NN}} = 5.02$ TeV is presented in this article. The measurements are carried out at midrapidity ($|y| < 0.5$) as a function of collision centrality using the ALICE detector. The p_{T}-integrated yields, the coalescence parameters and the ratios to protons and antiprotons are reported and compared with nucleosynthesis models. The comparison of these results in different collision systems at different center-of-mass collision energies reveals a suppression of nucleus production in small systems. In the Statistical Hadronisation Model framework, this can be explained by a small correlation volume where the baryon number is conserved, as already shown in previous fluctuation analyses. However, a different size of the correlation volume is required to describe the proton yields in the same data sets. The coalescence model can describe this suppression by the fact that the wave functions of the nuclei are large and the fireball size starts to become comparable and even much smaller than the actual nucleus at low multiplicities.

DOI: 10.1103/PhysRevC.107.064904

I. INTRODUCTION

Collisions of ultrarelativistic heavy ions create suitable conditions for the production of light (anti)nuclei, as a high energy density is reached over a large volume. Under these conditions, hot and dense matter, which contains approximately equal numbers of quarks and antiquarks at midrapidity, is produced for a short duration (a few 10^{-23} s). After a deconfined quark-gluon plasma (QGP) is formed in the initial state, the system cools down and undergoes a transition to a hadron gas. While the hadronic yields are fixed at the moment when the rate of inelastic collisions becomes negligible (chemical freeze-out), the transverse momentum (p_{T}) distributions continue to change until elastic interactions cease (kinetic freeze-out). The observed nucleus abundance is highly sensitive to the chemical freeze-out conditions as well as the dynamics of the emitting source.

The production of light nuclei and antinuclei has already been measured in many experiments at various energies in heavy-ion collisions at the Bevalac [1], the Schwerionensynchrotron (SIS) [2,3], the Alternating Gradient Synchrotron (AGS) [4–8], the Super Proton Synchrotron (SPS) [9–12], the Relativistic Heavy Ion Collider (RHIC) [13–20], and the Large Hadron Collider (LHC) [21–25], and in smaller collision systems [22,26–38]. The production of light nuclei is usually discussed within two theoretical approaches: the nucleon coalescence model [39–44] and the statistical hadronization model (SHM) [45–49].

Generally, the coalescence model describes the production of nuclei from the nucleons emitted from a hot fireball that cools down while expanding. Most variants use a phase-space picture for the formation; namely the nucleons have to be close in space and (relative) momentum to allow for the formation of the nucleus. In particular, the studies of the production of (anti)nuclei as a function of the charged-particle multiplicity [22] have clearly shown experimentally a dependence of the yield (ratios) on the volume of the emitting fireball. In fact, a strong suppression of nucleus-to-proton yield ratios is seen from high multiplicities in Pb-Pb to lower multiplicities in p-Pb, and reaching small multiplicities in pp [37,38] collisions. The size of the fireball can be extracted from the measurement of two-particle correlations, of Hanbury Brown–Twiss type [50–52], nowadays often called femtoscopy. Empirically, it was found that the charged-particle multiplicity of the collision is proportional to the size parameter R cubed [44,53]. Theoretically, these correlations can be directly connected to the coalescence parameter B_A, which is a measure for the probability to form a nucleus of mass number A from the corresponding nucleons [40–42,44,54–56]. This dependence is mainly given by the fact that the wave functions of the nucleons have to overlap with the nucleus's wave function, while the constituents are being emitted from a region of homogeneity of the fireball. This leads to a strong suppression of nucleus production in small systems, since the size of the formed nucleus becomes larger than the emitting source [44,57]. It is worthwhile to mention that coalescence models typically ignore the problem of conservation of energy and momentum in the process, assuming either that this is handled via the off-shell nature of the particles or additional particles involved in the process itself.

The SHM successfully describes hadron yields in heavy-ion collisions, in particular in central collisions and at

*Full author list given at the end of the article.

midrapidity [48]. The production of nuclei is solely determined by their quantum numbers and masses [49]. For more peripheral heavy-ion collisions or even smaller collision systems such as pp and p-Pb, one needs to switch from a grand canonical ensemble to a canonical description of the relevant quantum numbers (baryon number B, charge Q, and strangeness S) [58,59]. The canonical ensemble requires a local conservation of each quantum number in a particular volume V_c, the so-called correlation volume. Interestingly, V_c cannot be unambiguously determined from first principles [60], but it can be constrained from measurements of the event-by-event number fluctuation of net protons [59,61] or deuterons [25]. Other approaches include a nonequilibrium treatment of the quantum numbers in question (see Ref. [49] and references therein) or even a partial chemical equilibrium (PCE) [62–64].

In this article, the production of deuterons, tritons and ^{3}He and their antiparticles in Pb-Pb collisions at a center-of-mass energy per nucleon pair $\sqrt{s_{NN}} = 5.02$ TeV is reported. The p_T-integrated yields, the coalescence parameters (calculated using average of protons and antiprotons, since they are found to be produced in same abundance at the LHC energies [65]) and the ratios to protons and antiprotons are compared with nucleon coalescence and statistical hadronization models.

II. EXPERIMENTAL APPARATUS AND DATA SAMPLE

The results presented in this article are based on the data set of Pb-Pb collisions at $\sqrt{s_{NN}} = 5.02$ TeV collected in 2018. In total, 230×10^6 events were analyzed, of which 86.7×10^6 are central trigger events in the 0–10% centrality interval and 74.3×10^6 are semicentral trigger events in the 30–50% centrality interval.

The ALICE detector [66,67] has excellent particle identification and vertexing capabilities. The (anti)nuclei were measured using the Inner Tracking System (ITS), the Time Projection Chamber (TPC) and the time-of-flight (TOF) detector. All these detectors are located inside a homogeneous magnetic field with a strength of 0.5 T and cover the full azimuthal acceptance and the pseudorapidity range $|\eta| < 0.9$ for interactions located in $|z| < 10$ cm, where z is the distance from the nominal interaction point along the beam direction.

The ITS [68] consists of six cylindrical layers of (position-sensitive) silicon detectors, covering the central rapidity region. The ITS allows the reconstruction of the primary and secondary vertices. It is also used to separate primary nuclei from secondary nuclei via the distance of closest approach (DCA) of the track to the primary vertex with good resolution (better than 300 μm), assured by the Silicon Pixel Detector (SPD), which comprises the innermost two layers of the ITS.

The TPC [69] is the main tracking device of the experiment. It is a gas-filled cylinder and provides particle identification via the specific energy loss (dE/dx). (Anti)^{3}He are identified up to $p_T = 7$ GeV/c using the TPC only.

The TOF detector [70] allows for the light (anti)nuclei identification by means of the velocity determination. Its total time resolution for tracks from Pb-Pb collisions corresponds to about 65 ps which is determined by the intrinsic time resolution of the detector and the resolution of the event collision time measurement. By a combined analysis of TPC and TOF data, (anti)deuterons are identified up to $p_T = 6$ GeV/c in Pb-Pb collisions. (Anti)tritons are also identified using TPC and TOF. However, due to a sizable background starting at about 2 GeV/c originating from mismatches between a track and a cluster in TOF, the (anti)tritons can only be measured up to $p_T = 3.2$ GeV/c in this data set.

The Transition Radiation Detector (TRD) [71] was designed to provide electron identification and triggering and to improve the track reconstruction and calibration in the central barrel of ALICE. The TRD improves the overall momentum resolution of the ALICE central barrel by providing additional space points at large radii for tracking, reducing as well significantly the probability of mismatch between tracks and TOF hits for rare probes analyses such as the triton analysis presented in this article.

Finally, a pair of forward and backward scintillator hodoscopes ($2.8 < \eta < 5.1$ and $-3.7 < \eta < -1.7$), the V0 detectors [72], measures the arrival time of particles with a resolution of 1 ns. The V0 detectors are used for triggering purposes and for rejection of beam-gas interactions. Furthermore, it provides the centrality determination in Pb-Pb collisions.

III. DATA ANALYSIS

A. Event and track selection

The data were collected using a minimum-bias trigger requiring at least one hit in both the V0 detectors. In addition, a central and a semicentral trigger were used, also determined by the V0 detectors, selecting collisions in the 0–10% and 30–50% centrality intervals, respectively. Moreover, the timing information of the V0 scintillator arrays is used to reject the events triggered by the interactions of the beam with the residual gas in the LHC vacuum pipe. A further selection using a zero degree calorimeter is applied in order to reject the electromagnetic beam-beam interactions and beam-satellite bunch collisions [73]. These three rejections are done in the offline analysis.

The production yield of primary (anti)deuterons, (anti)tritons and (anti)^{3}He are measured at midrapidity. In order to provide optimal particle identification by reducing the difference between transverse and total momentum, the spectra are provided within a rapidity window of $|y| < 0.5$. Only tracks in the full tracking acceptance of $|\eta| < 0.8$ are selected. In order to guarantee good track momentum and dE/dx resolution in the relevant p_T ranges, the selected tracks are required to have at least 70 out of 159 possible reconstructed points in the TPC and two points in the ITS (out of which at least one is in the SPD). The requirement of at least one point in the two innermost layers, the SPD, assures a resolution better than 300 μm on the distance of closest approach to the primary vertex in the planes perpendicular (DCA_{xy}) and parallel (DCA_z) to the beam axis for the selected tracks [67]. Furthermore, it is required that the χ^2 per TPC reconstructed point is less than 2.5 and tracks of weak-decay

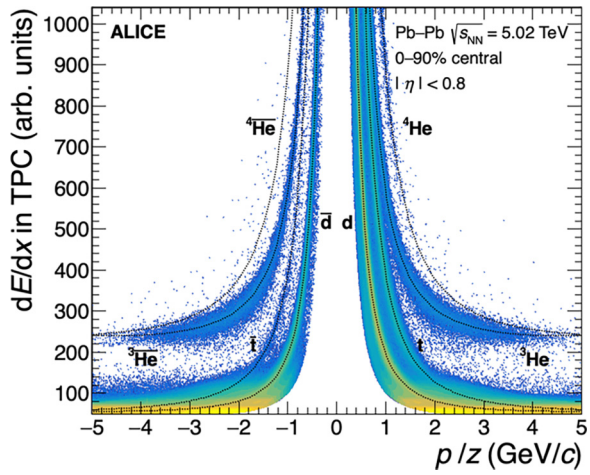

FIG. 1. Specific energy loss of charged tracks in the TPC vs rigidity (p/z) for Pb-Pb collisions at $\sqrt{s_{NN}} = 5.02$ TeV. The dashed lines represent parametrizations of the Bethe-Bloch curve. Particles lighter than deuterons have been removed by applying a selection in the dE/dx vs p/z plane that corresponds to the upper edge (3σ) of the proton band such that only nuclei are visible.

products are rejected as they cannot originate from the tracks of primary nuclei.

B. Particle identification

The TPC allows for a clean identification of (anti)^{3}He in the whole p_{T} range and of (anti)deuterons up to $p_{\mathrm{T}} \approx 1$ GeV$/c$. For higher transverse momenta, the dE/dx information for charged particles is combined with the TOF mass determination in the (anti)deuteron analysis. For the (anti)tritons in the whole p_{T} range, a combined TPC and TOF analysis is performed. Figure 1 shows the TPC specific energy loss as a function of rigidity (p/z) in Pb-Pb collisions at $\sqrt{s_{NN}} = 5.02$ TeV. The dashed curves represent parametrizations of the Bethe-Bloch formula for the different particle species. The (anti)deuteron and (anti)^{3}He identification with the TPC is achieved by requiring that the energy-loss signal of a track lies in a 3σ window around the expected value for a given mass hypothesis, where σ is the dE/dx resolution. For the (anti)tritons, a reduced 2σ window is employed in order to further decrease the background.

In order to extend the p_{T} reach of the measurement, it is additionally required that the track is matched to a hit in the TOF detector. As shown in Fig. 2, based on the time-of-flight measurement the squared mass of the particle is determined in different p_{T} intervals and the distributions are then fitted using a Gaussian function with an exponential tail for the signal. The background of the (anti)deuterons mainly originates from two components, namely wrong association of a track with a TOF hit and the non-Gaussian tail of lower mass particles. For the (anti)tritons the dominant background originates from the wrong associations of a track with a TOF hit. For both nuclei, the background is described with the sum of two exponential functions.

C. Background rejection

Among of the main sources of background in the analyses of the primary deuteron and triton production are nuclei originating from secondary interactions. These secondary nuclei come mostly from the interactions of other primary particles with the detector material. In some of these interactions, a light nucleus can be produced by spallation processes, i. e., can be knocked out from detector or from support material. The baryon number conservation sets a very high energy threshold for the production of secondary antinuclei with similar processes, thus making the contribution of secondary antinuclei from material negligible, as also confirmed by simulations. Other processes, such as the decay of (anti)hypernuclei, represent a negligible contamination of the observed (anti)deuterons and (anti)tritons.

As already done in previous analyses [21–25], in order to subtract the background from secondary deuterons and ^{3}He the DCA$_{xy}$ is used. The distribution of primary particles is expected to be peaked at DCA$_{xy} = 0$, whereas secondary particles are expected to exhibit a flat DCA$_{xy}$ distribution to the

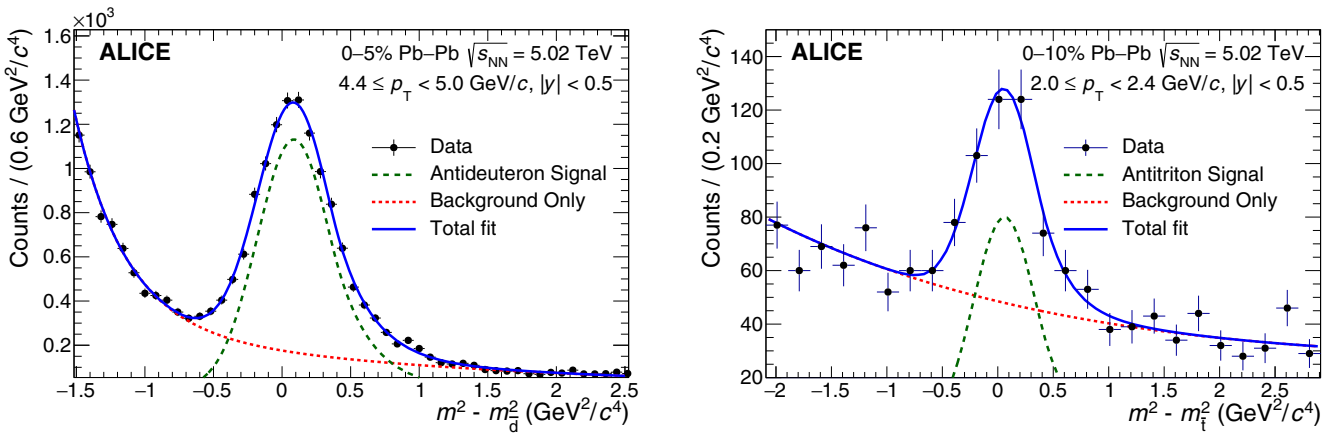

FIG. 2. Fit to the measured squared mass to extract the antideuteron signal in $4.4 < p_{\mathrm{T}} < 5.0$ GeV$/c$ (left) and the antitriton signal in $2.0 < p_{\mathrm{T}} < 2.4$ GeV$/c$ (right). The red dashed line shows the background, the solid blue line the combined fit to the data, and the green dashed line the signal only.

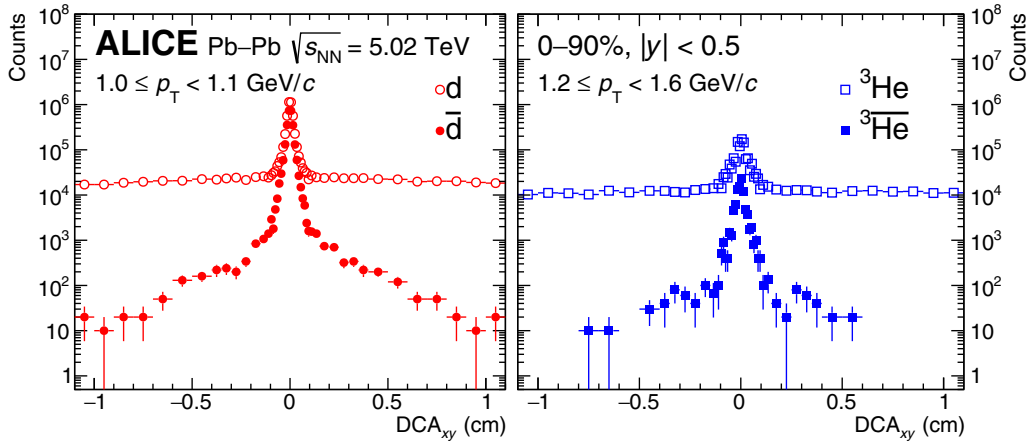

FIG. 3. DCA$_{xy}$ of deuterons (open red circles) and antideuterons (solid red circles) for the p_T intervals $1.0 \leqslant p_T < 1.1$ GeV/c (left) and of ^{3}He (open blue squares) and $^3\overline{\text{He}}$ (solid blue squares) for $1.2 \leqslant p_T < 1.6$ GeV/c (right).

first order. The typical distributions of DCA$_{xy}$ for nuclei and antinuclei detected in ALICE are shown in Fig. 3. In second order, the tracks originating from secondary particles may be associated to a wrong hit in the innermost layers of the ITS. If the latter belongs to a primary particle, the extrapolation of the secondary particle track will wrongly point to the primary vertex, as the track pointing is mostly driven by the hits in the innermost layers of the ITS. In the deuteron and ^{3}He analyses presented in this article, a fit to the observed DCA$_{xy}$ distribution is performed to extract the primary fraction of deuterons and ^{3}He. The DCA$_{xy}$ distributions of primary and secondary deuterons as well as ^{3}He in each transverse momentum interval are extracted from Monte Carlo (MC) events and are used as templates to fit the measured DCA$_{xy}$ distribution. Since the secondary particles have large DCA$_{xy}$, the fits are done in a range of DCA$_{xy}$ wider than the actual track selection criterion to better constrain the secondary particle components. The contamination from deuterons produced in the interactions with the detector material is only significant below 1.4 GeV/c.

In contrast to deuterons, the background from secondary tritons is rather dominant over the low number of primary triton counts. As this background only occurs at low p_T, the triton yield is only measured above 2.4 GeV/c (2.0 GeV/c in the most peripheral centrality interval).

D. Corrections to the spectra

The p_T-differential-production spectra of (anti)deuterons, (anti)^{3}He, and (anti)tritons are obtained by correcting the raw spectra for tracking efficiency and acceptance based on MC generated events. The MC samples used to compute the efficiency and the acceptance corrections for the Pb-Pb analysis were generated using the HIJING event generator [74]. Since HIJING does not provide light (anti)nuclei, an *ad hoc* generator that injects particles on top of the event generator was used. The kinematics of the injected nuclei is chosen randomly by picking their transverse momentum from a flat distribution in the range between 0 and 10 GeV/c, their azimuthal angle from a flat distribution between 0 and 2π radians, and their rapidity from a flat distribution in the range $|y| < 1$. All particles are transported with GEANT4 [75] through a full simulation of the ALICE detector. The GEANT4 version used in the ALICE software framework was modified to take into account the latest (anti)nuclei hadronic interaction measurements [24,76].

For the (anti)deuteron, (anti)^{3}He, and (anti)triton analyses, the efficiency×acceptance was determined for each centrality interval separately. The input p_T distributions of (anti)nuclei in the simulation are modified according to a blast-wave (BW) parametrization using p_T -dependent weights. The BW parameters are taken from [65].

IV. SYSTEMATIC UNCERTAINTIES

The sources of systematic uncertainties affecting these measurements were studied as follows:

(1) the amount of material budget employed in the MC simulation of the ALICE apparatus was varied by ± 4.5%, corresponding to the uncertainty on the ALICE material budget determination [67];
(2) track selection criteria were varied as done for previous analyses [21–25];
(3) fit functions used for the signal extraction were varied;
(4) for the antitriton analysis different functions were used to weight the input spectra in the simulation.

A large contribution of the systematic uncertainty is due to the limited knowledge of the interaction of nuclei with the detector material. The main transport code used in ALICE is GEANT4 [75]. This is used to estimate the efficiency×acceptance that is applied as correction to the spectra. In general, the accuracy of the transport codes is limited by the available data for nuclei and especially (anti)nuclei hadronic interaction cross sections, which have only been measured in energy ranges far from the typical momenta of light (anti)nuclei produced in heavy-ion collisions [77–80]. In a detailed study comparing the available data on different targets and their description in GEANT4, the corresponding uncertainty is evaluated as the scaling factor for the cross section value in GEANT4 that is required to match the experimental data. The simulations to estimate the efficiency are

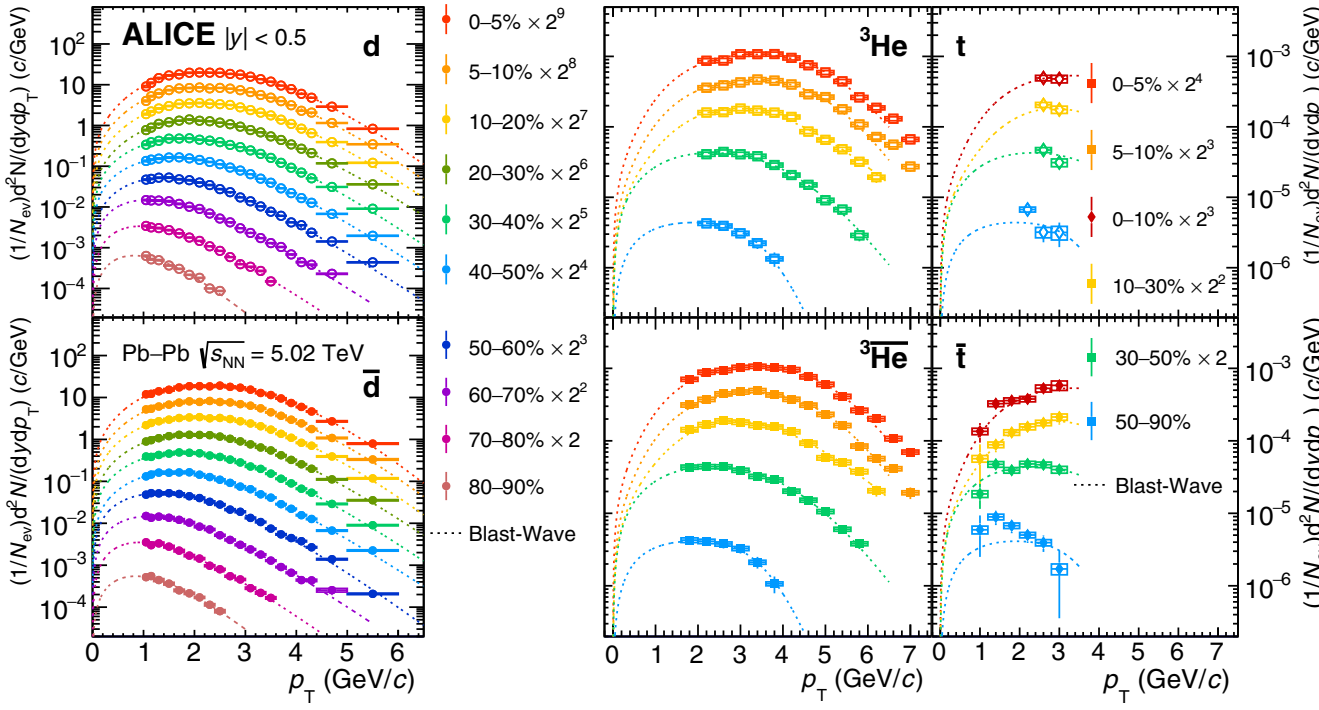

FIG. 4. (Anti)deuteron, (anti)^{3}He, and (anti)t spectra measured in Pb-Pb collisions at $\sqrt{s_{NN}} = 5.02$ TeV for different centrality classes reported with different colours. The boxes represent the systematic uncertainties, while the vertical lines are the statistical ones. The dashed lines represent the individual blast-wave fits to the spectra. The blast-wave fits of (anti)^{3}He are used on (anti)t spectra as well to show the trend.

then repeated with the cross section in GEANT4 scaled by this factor. The determined systematic uncertainty is below 1% for the deuterons using TPC and TOF and about 8% for antideuterons at low p_T, and decreases down to 4% at the largest p_T. For ^{3}He it is about 0.5% and for $^3\overline{\text{He}}$ it is about 2% with a small dependence on p_T. The values for t and $\bar{t}$ are similar, with about 0.5% and between 2.5% and 5%, respectively. In addition, weak decays from (anti)hypertritons can affect the (anti)^{3}He spectra and contribute to the systematic uncertainties with about 1.7%. The discrepancy between the data and MC description of the ITS-TPC matching efficiencies is accounted for by adding 5% of systematic uncertainties. All the other systematic uncertainties in the Pb-Pb analyses were estimated separately for each centrality class: particle identification and analysis selection criteria contribute by less than 3%; the signal extraction method by less than 2%; the TPC particle identification systematic uncertainty is estimated to be less than 2%.

The huge background and the low number of counts of the (anti)triton analysis result in quite large statistical uncertainties, and the systematic variations were found to be not significant within the statistical uncertainties. Therefore, the uncertainties from the variations were dropped and instead systematic uncertainties based on similar studies for charged pions, kaons, and protons were assigned, namely 5% for the ITS-TPC matching efficiency and 6% for the signal extraction for all centrality and p_T intervals. The uncertainty on the p_T spectra coming from the uncertainty of the ALICE material budget was determined to be 2% [24]. For the weighting of the efficiency×acceptance, various functional dependencies were applied. This results in a negligible uncertainty in the higher p_T intervals, where the weighting does not have any effect, and up to 8% uncertainty in the lower p_T intervals. To evaluate the systematic uncertainty due to the background estimation, an alternative data-driven method was used to determine the background. In this method, nontriton candidates were selected in the TPC by requiring that their dE/dx is outside a $\pm 2\sigma$ window around the triton peak. Their squared TOF-mass distribution is used as a template for the background, which is scaled to the squared TOF-mass distribution of triton candidates. It matches very well the background outside the triton peak region and allows an independent estimate of the background under the triton peak. This results in no systematic uncertainty in the low p_T region without any background and up to 20% in the higher p_T intervals. All these contributions result in a total systematic uncertainty for the (anti)triton p_T spectra between 8% and 22%.

V. RESULTS

The transverse momentum spectra of (anti)deuterons, (anti)^{3}He, and (anti)tritons are extracted in Pb-Pb collisions at $\sqrt{s_{NN}} = 5.02$ TeV for various centrality classes. The transverse momentum spectra are shown in Fig. 4. A clear evolution of the spectral shape with centrality is observed, with the average transverse momentum almost doubling its value going from peripheral to most central Pb-Pb collisions and a shift in the peak position towards higher p_T for increasing multiplicity.

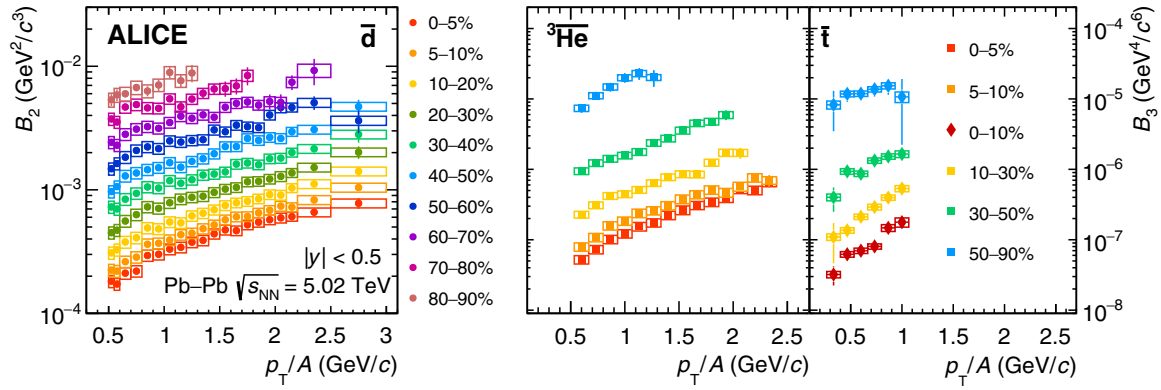

FIG. 5. Coalescence parameters B_2 (left) and B_3 (right) measured for antinuclei in Pb-Pb collisions at $\sqrt{s_{NN}} = 5.02$ TeV as a function of the transverse momentum scaled by the mass number. Compatible results are obtained for the nuclei. Each color corresponds to a different centrality class. The boxes represent the systematic uncertainties, while the vertical lines are the statistical ones. See the text for details.

In order to measure the total yield per rapidity unit in Pb-Pb collisions, the spectra were fitted with the blast-wave function, which assumes a thermal production of particles from an expanding source [81]. The systematic uncertainty of the integrated yield is obtained by shifting the spectrum within its systematic uncertainties and adding an additional uncertainty quadratically to account for the extrapolation to low and high p_T. The latter is estimated by using different fit functions such as the m_T exponential, Boltzmann, Fermi-Dirac, and Bose-Einstein functions [82]. The fractions of extrapolated yield at low p_T for different centrality classes are about 5% to 40% for (anti)deuterons, 15% (8%) to 50% (35%) for (anti)^{3}He, and 23% (1%) to 50% (11%) for (anti)tritons depending on the centrality class. The extrapolated yields in the high-p_T region are negligible for most of the centrality classes except for a 3% contribution for the most peripheral collisions for (anti)deuterons and (anti)^{3}He, and a 55% to 15% contribution depending on the centrality class for (anti)tritons. The statistical uncertainties are calculated by repeating the blast-wave fit by shifting the spectra randomly with a Gaussian distribution within the statistical uncertainties of each p_T interval. The resulting yield distribution is fitted with a Gaussian and the width of this distribution is taken as the statistical uncertainty.

The coalescence scenario can be tested by computing the coalescence parameter B_A (see for instance Ref. [83] and references therein). Under the assumption of equal production of protons and neutrons, it is defined as

$$B_A = E_A \frac{d^3N_A}{dp_A^3} \left(E_p \frac{d^3N_p}{dp_p^3} \right)^{-A}, \quad (1)$$

where $E_A \frac{d^3N_A}{dp_A^3}$ and $E_p \frac{d^3N_p}{dp_p^3}$ are the invariant production spectra of the nuclei with mass number A and of protons, respectively. Protons are used here since neutrons are unmeasured and isospin symmetry is expected at LHC energies. Figure 5 shows the measured coalescence parameters B_2 and B_3 as a function of the transverse momentum scaled by the mass number A for Pb-Pb collisions at $\sqrt{s_{NN}} = 5.02$ TeV. An ordering of the coalescence parameters with collision centrality, from higher B_A values in peripheral collisions to lower B_A values in the central ones is clearly visible. This trend with centrality is explained in the coalescence model framework as a consequence of the increasing radius R of the source from peripheral to central events [44,56,57]. Similarly, the decrease of R with increasing momentum as measured with two-proton correlations [84] can also explain the increase of the coalescence parameters with momentum observed in Fig. 5, as already seen in small collision systems [37]. Notably, the space-momentum correlations between nucleons restrict the volume that is effectively used for coalescence and make it smaller than the total volume. This means that particles at higher momentum probe a smaller region in the radially expanding system.

The ratio between the production yields of $^3\overline{He}$ and $\bar{t}$ provides another powerful test of the coalescence predictions [57]. This model gives two predictions for the formation: one assumes that the $A = 3$ nuclei are formed from three nucleons (called three-body coalescence in the following) and the other assumes the formation of the nucleus from a deuteron and a nucleon (two-body coalescence). Figure 6 shows on the left the measured ratios as a function of transverse momentum in different centrality classes. The ratios are flat with p_T within uncertainties. The average ratio $\bar{t}\,/^3\overline{He}$ over the measured transverse momenta is shown in Fig. 6 on the right, as a function of the charged-particle multiplicity $\langle dN_{ch}/d\eta \rangle$ determined in a pseudorapidity range of $|\eta_{lab}| < 0.5$ in the laboratory system. While the SHM expectation for this ratio is very close to 1, the predictions from the coalescence model [57] deviate from unity due to the difference in the wave functions of the two nuclei. However, within the current statistical and systematic uncertainties, it is not possible to conclude which flavor of coalescence model is favoued by the measurement, nor if there is any significant departure from the SHM expectations.

Figure 7 shows the measured d/p, ^{3}He$/p$, and t/p for different collision systems at different energies. Both the coalescence models (using the two different approaches, i. e., two-body and three-body coalescence [57], and on top of URQMD [85,86]) and the canonical SHM (CSM) [58]

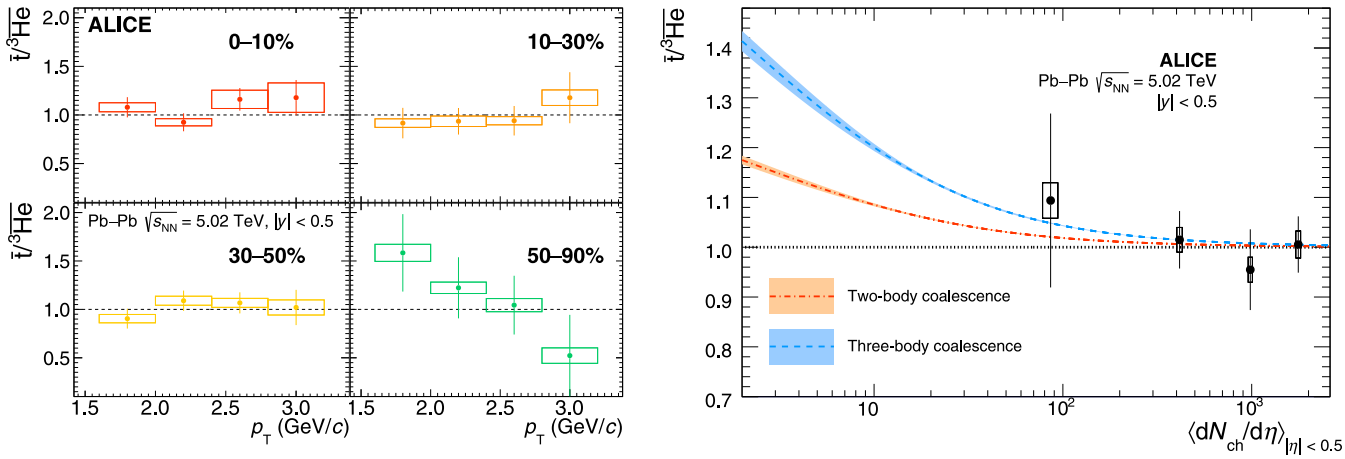

FIG. 6. Left: ratios of transverse momentum spectra of $\bar{t}$ and $^3\overline{\text{He}}$ in different centrality intervals. Right: multiplicity dependence of the average $\bar{t}$ /$^3\overline{\text{He}}$ ratio compared with the coalescence model expectations (two-body coalescence in orange and three-body coalescence in blue) [57]. The open boxes represent the total systematic uncertainties, while the vertical lines are the statistical ones.

capture qualitatively the observed trend with multiplicity. The UrQMD model uses a hybrid approach where nuclei are ultimately produced by coalescence. However, none of the model curves are able to explain quantitatively all the data points. In all cases, a decrease in the ratios is observed from central Pb-Pb collisions toward peripheral Pb-Pb collisions. In particular, in the case of the d/p ratio, this depletion is significant when considering only the uncorrelated uncertainties. Such an effect is expected in transport codes modeling interactions of the nuclei in the rescattering phase following the hadron formation [85].

In the SHM, assuming the grand canonical ensemble, the nucleus-to-proton ratios are fixed by the temperature of the source, thus they are expected to stay constant as a function of charged-particle multiplicity. However, when assuming a canonical ensemble and the exact conservation of baryon number over a defined volume, the nucleus-to-proton ratios increase from low to high multiplicities. The extension of the conservation volume was studied via event-by-event correlation measurement and it was found to be $V_c = (1.6 \pm 0.2)\, dV/dy$ [25]. The studies presented here thus show that a small conservation volume is needed to describe deuteron-to-

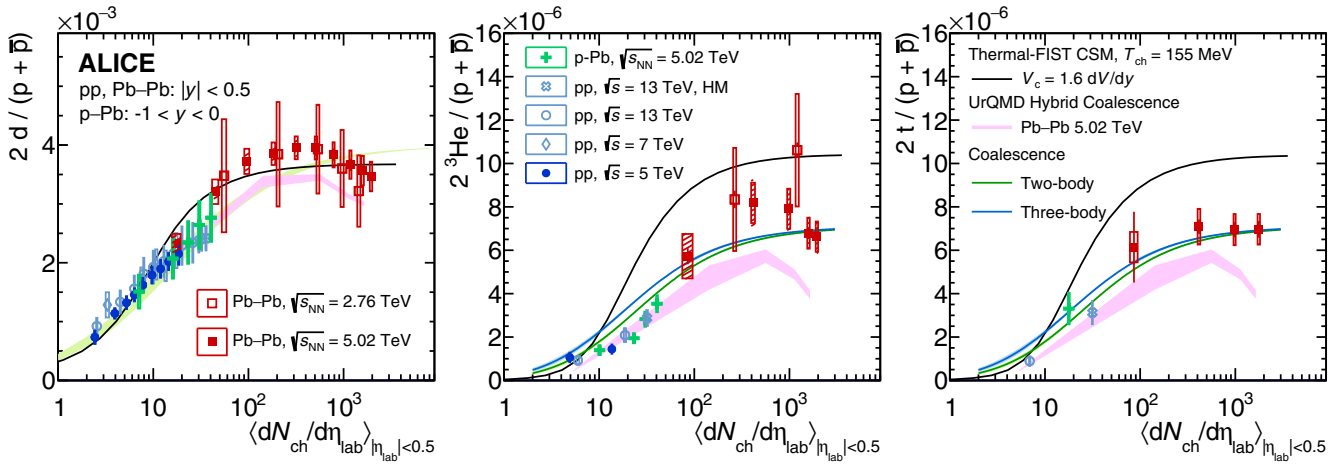

FIG. 7. Integrated deuteron (left), ^{3}He (middle), and triton yields (right) over proton yields as a function of charged-particle multiplicity $\langle dN/d\eta_{ch} \rangle$ for pp, p-Pb, and Pb-Pb collisions measured by the ALICE Collaboration. The boxes represent the uncorrelated systematic uncertainties, while the vertical lines are the statistical ones. The shaded boxes represent the centrality-correlated uncertainties. In addition, the data are compared to the THERMAL-FIST CSM (canonical statistical model) at 155 MeV with a correlation volume of $V_c = 1.6\, dV/dy$ shown as a black line [58], the two coalescence approaches displayed in green (two-body coalescence) and in blue (three-body coalescence) [57], and URQMD hybrid coalescence shown as a purple line [86].

proton ratio in peripheral Pb-Pb collisions within the SHM, while the production of protons requires significantly larger values of around $V_c = (3\text{–}5)\, dV/dy$ [61]. At the moment, there is no configuration of the SHM that is able to describe simultaneously protons and nuclei with a single set of parameters in peripheral Pb-Pb and smaller collision systems. The decrease of the nucleus over proton ratios going towards smaller multiplicities is also expected in coalescence models, where it is caused by the evolution of the system size with multiplicity.

VI. SUMMARY AND CONCLUSION

In this article, we have presented comprehensive measurements of the production of (anti)nuclei in Pb-Pb collisions at $\sqrt{s_{NN}} = 5.02$ TeV including the first antitriton measurement in Pb-Pb collisions at LHC energies. The obtained results follow the trends established at lower collision energy, but show a much larger constraining power on models thanks to significantly smaller systematic and statistical uncertainties.

For deuterons, the number of studied centrality intervals was largely increased compared to previous ALICE studies and demonstrate the strong increase of the radial flow when going from peripheral to central events. This is similarly visible for ^{3}He and t, but with a lower number of centrality intervals. The extracted spectra for t and ^{3}He agree well in the overlap region of both spectra. Only for the most peripheral interval a slight deviation from unity is visible, which is also expected by coalescence models, where the deviation at low multiplicities is expected due to the different spatial wave functions of t and ^{3}He [44,57]. This will be constrained better with high-statistics data from Run 3, using all available collision systems, i. e., *pp*, *p*-Pb, and Pb-Pb.

The yield ratios of d/p as a function of charged-particle multiplicity agree well with both expectations, i. e., coalescence and thermal models. Notably, the deuteron-over-proton ratio requires a small correlation volume within the SHM with respect to net-proton fluctuation measurements. For ^{3}He the data lie at low multiplicity slightly closer to the coalescence expectations, and for high multiplicities corresponding to Pb-Pb the data lie between thermal and coalescence models. In contrast, for the triton the data points are much closer to the coalescence model with multiplicities in Pb-Pb collisions. Recently, several works appeared [87–89] that each try to improve the SHM in particular multiplicity regions. They give a good description in the region they are applied to, but they are not applicable in the full multiplicity range investigated here.

The presented data, even though they are much more precise than previous results, still do not allow for a strong conclusion about the dominant production mechanism. More differential studies, in particular also those involving additional (hyper)nuclei, such as ^{4}He and $^3_\Lambda$H, will help us to understand better the processes underlying the formation of composite objects.

The ongoing Run 3 of the LHC with the upgraded ALICE apparatus will allow for such more precise studies of (anti)(hyper)nuclei production and for the extension to mass $A = 4$ hypernuclei in Pb-Pb collisions [90].

ACKNOWLEDGMENTS

The ALICE Collaboration would like to thank all its engineers and technicians for their invaluable contributions to the construction of the experiment and the CERN accelerator teams for the outstanding performance of the LHC complex. The ALICE Collaboration gratefully acknowledges the resources and support provided by all Grid centres and the Worldwide LHC Computing Grid (WLCG) Collaboration. The ALICE Collaboration acknowledges the following funding agencies for their support in building and running the ALICE detector: A. I. Alikhanyan National Science Laboratory (Yerevan Physics Institute) Foundation (ANSL), State Committee of Science, and World Federation of Scientists (WFS), Armenia; Austrian Academy of Sciences, Austrian Science Fund (FWF) [M 2467-N36] and Nationalstiftung für Forschung, Technologie und Entwicklung, Austria; Ministry of Communications and High Technologies, National Nuclear Research Center, Azerbaijan; Conselho Nacional de Desenvolvimento Científico e Tecnológico (CNPq), Financiadora de Estudos e Projetos (Finep), Fundação de Amparo à Pesquisa do Estado de São Paulo (FAPESP), and Universidade Federal do Rio Grande do Sul (UFRGS), Brazil; Bulgarian Ministry of Education and Science, within the National Roadmap for Research Infrastructures 2020–2027 (object CERN), Bulgaria; Ministry of Education of China (MOEC), Ministry of Science & Technology of China (MSTC), and National Natural Science Foundation of China (NSFC), China; Ministry of Science and Education and Croatian Science Foundation, Croatia; Centro de Aplicaciones Tecnológicas y Desarrollo Nuclear (CEADEN), Cubaenergía, Cuba; Ministry of Education, Youth and Sports of the Czech Republic, Czech Republic; The Danish Council for Independent Research–Natural Sciences, the VILLUM FONDEN, and Danish National Research Foundation (DNRF), Denmark; Helsinki Institute of Physics (HIP), Finland; Commissariat à l'Energie Atomique (CEA) and Institut National de Physique Nucléaire et de Physique des Particules (IN2P3) and Centre National de la Recherche Scientifique (CNRS), France; Bundesministerium für Bildung und Forschung (BMBF) and GSI Helmholtzzentrum für Schwerionenforschung GmbH, Germany; General Secretariat for Research and Technology, Ministry of Education, Research and Religions, Greece; National Research, Development and Innovation Office, Hungary; Department of Atomic Energy Government of India (DAE), Department of Science and Technology, Government of India (DST), University Grants Commission, Government of India (UGC), and Council of Scientific and Industrial Research (CSIR), India; National Research and Innovation Agency–BRIN, Indonesia; Istituto Nazionale di Fisica Nucleare (INFN), Italy; Japanese Ministry of Education, Culture, Sports, Science and Technology (MEXT) and Japan Society for the Promotion of Science (JSPS) KAKENHI, Japan; Consejo Nacional de Ciencia (CONACYT) y Tecnología, through Fondo de Cooperación Internacional en Ciencia y Tecnología (FONCICYT) and Dirección General de Asuntos del Personal Academico (DGAPA), Mexico; Nederlandse Organisatie voor Wetenschappelijk Onderzoek (NWO), Netherlands; The Research Council of Norway, Norway; Commission on Science

and Technology for Sustainable Development in the South (COMSATS), Pakistan; Pontificia Universidad Católica del Perú, Peru; Ministry of Education and Science, National Science Centre and WUT ID-UB, Poland; Korea Institute of Science and Technology Information and National Research Foundation of Korea (NRF), Republic of Korea; Ministry of Education and Scientific Research, Institute of Atomic Physics, Ministry of Research and Innovation, and Institute of Atomic Physics and University Politehnica of Bucharest, Romania; Ministry of Education, Science, Research and Sport of the Slovak Republic, Slovakia; National Research Foundation of South Africa, South Africa; Swedish Research Council (VR) and Knut & Alice Wallenberg Foundation (KAW), Sweden; European Organization for Nuclear Research, Switzerland; Suranaree University of Technology (SUT), National Science and Technology Development Agency (NSTDA), Thailand Science Research and Innovation (TSRI), and National Science, Research and Innovation Fund (NSRF), Thailand; Turkish Energy, Nuclear and Mineral Research Agency (TENMAK), Turkey; National Academy of Sciences of Ukraine, Ukraine; Science and Technology Facilities Council (STFC), United Kingdom; National Science Foundation of the United States of America (NSF) and United States Department of Energy, Office of Nuclear Physics (DOE NP), United States of America. In addition, individual groups or members have received support from Marie Skłodowska Curie, European Research Council, Strong 2020–Horizon 2020 (Grants No. 950692, No. 824093, No. 896850), European Union; Academy of Finland (Center of Excellence in Quark Matter) (Grants No. 346327, No. 346328), Finland; Programa de Apoyos para la Superación del Personal Académico, UNAM, Mexico.

[1] S. Nagamiya, M. C. Lemaire, E. Moeller, S. Schnetzer, G. Shapiro, H. Steiner, and I. Tanihata, Production of pions and light fragments at large angles in high- nuclear collisions, Phys. Rev. C **24**, 971 (1981).

[2] W. Reisdorf *et al.* (FOPI Collaboration), Systematics of central heavy ion collisions in the 1*A* GeV regime, Nucl. Phys. A **848**, 366 (2010).

[3] J. Adamczewski-Musch *et al.* (HADES Collaboration), Directed, Elliptic, and Higher Order Flow Harmonics of Protons, Deuterons, and Tritons in Au+Au Collisions at $\sqrt{s_{NN}} =$ 2.4 GeV, Phys. Rev. Lett. **125**, 262301 (2020).

[4] N. Saito *et al.* (E886 Collaboration), Composite particle production in relativistic Au+Pt, Si+Pt, and p+Pt collisions, Phys. Rev. C **49**, 3211 (1994).

[5] T. A. Armstrong *et al.* (E864 Collaboration), Measurements of light nuclei production in 11.5*A* GeV/c Au+Pb heavy-ion collisions, Phys. Rev. C **61**, 064908 (2000).

[6] T. A. Armstrong *et al.* (E864 Collaboration), Antideuteron Yield at the AGS and Coalescence Implications, Phys. Rev. Lett. **85**, 2685 (2000).

[7] S. Albergo *et al.*, Light nuclei production in heavy-ion collisions at relativistic energies, Phys. Rev. C **65**, 034907 (2002).

[8] M. J. Bennett *et al.* (E878 Collaboration), Light nuclei production in relativistic Au + nucleus collisions, Phys. Rev. C **58**, 1155 (1998).

[9] J. Simon-Gillo *et al.* (NA44 Collaboration), Deuteron and antideuteron production in CERN experiment NA44, Nucl. Phys. A **590**, 483 (1995).

[10] S. V. Afanasiev *et al.* (NA49 Collaboration), Deuteron production in central Pb+Pb collisions at 158*A* GeV, Phys. Lett. B **486**, 22 (2000).

[11] T. Anticic *et al.* (NA49 Collaboration), Energy and centrality dependence of deuteron and proton production in Pb+Pb collisions at relativistic energies, Phys. Rev. C **69**, 024902 (2004).

[12] R. Arsenescu *et al.* (NA52 Collaboration), An Investigation of the anti-nuclei and nuclei production mechanism in Pb + Pb collisions at 158*A* GeV, New J. Phys. **5**, 150 (2003).

[13] C. Adler *et al.* (STAR Collaboration), $\overline{d}$ and $^3\overline{\mathrm{He}}$ Production in $\sqrt{s_{NN}} = 130$ GeV Au + Au Collisions, Phys. Rev. Lett. **87**, 262301 (2001).

[14] S. S. Adler *et al.* (PHENIX Collaboration), Deuteron and Antideuteron Production in Au+Au Collisions at $\sqrt{s_{NN}} =$ 200 GeV, Phys. Rev. Lett. **94**, 122302 (2005).

[15] S. Afanasiev *et al.* (PHENIX Collaboration), Elliptic Flow for ϕ Mesons and (Anti)deuterons in Au + Au Collisions at $\sqrt{s_{NN}} =$ 200 GeV, Phys. Rev. Lett. **99**, 052301 (2007).

[16] B. Abelev *et al.* (STAR Collaboration), Yields and elliptic flow of $d(\bar{d})$ and $^3\mathrm{He}(^3\overline{\mathrm{He}})$ in Au+Au collisions at $\sqrt{s_{NN}} =$ 200 GeV, arXiv:0909.0566.

[17] STAR Collaboration, Observation of the antimatter helium-4 nucleus, Nature (London) **473**, 353 (2011).

[18] J. Adam *et al.* (STAR Collaboration), Beam energy dependence of (anti-)deuteron production in Au+Au collisions at the BNL Relativistic Heavy Ion Collider, Phys. Rev. C **99**, 064905 (2019).

[19] J. Adam *et al.* (STAR Collaboration), Beam-energy dependence of the directed flow of deuterons in Au+Au collisions, Phys. Rev. C **102**, 044906 (2020).

[20] M. Abdallah *et al.* (STAR Collaboration), Light nuclei collectivity from $\sqrt{s_{NN}} = 3$ GeV Au+Au collisions at RHIC, Phys. Lett. B **827**, 136941 (2022).

[21] J. Adam *et al.* (ALICE Collaboration), Precision measurement of the mass difference between light nuclei and anti-nuclei, Nat. Phys. **11**, 811 (2015).

[22] J. Adam *et al.* (ALICE Collaboration), Production of light nuclei and anti-nuclei in pp and Pb-Pb collisions at energies available at the CERN Large Hadron Collider, Phys. Rev. C **93**, 024917 (2016).

[23] S. Acharya *et al.* (ALICE Collaboration), Measurement of deuteron spectra and elliptic flow in Pb–Pb collisions at $\sqrt{s_{\mathrm{NN}}} = 2.76$ TeV at the LHC, Eur. Phys. J. C **77**, 658 (2017).

[24] The ALICE Collaboration, Measurement of anti-^{3}He nuclei absorption in matter and impact on their propagation in the Galaxy, Nat. Phys. **19**, 61 (2023).

[25] ALICE Collaboration, First measurement of antideuteron number fluctuations at energies available at the Large Hadron Collider, arXiv:2204.10166.

[26] B. Alper *et al.* (British-Scandinavian Collaboration), Large angle production of stable particles heavier than the proton and a

search for quarks at the CERN intersecting storage rings, Phys. Lett. B **46**, 265 (1973).
[27] W. M. Gibson *et al.* (British-Scandinavian-MIT Collaboration), Production of deuterons and antideuterons in proton-proton collisions at the CERN ISR, Lett. Nuovo Cimento **21**, 189 (1978).
[28] T. Alexopoulos *et al.* (Fermilab E735 Collaboration), Cross sections for deuterium, tritium, and helium production in $\overline{p}p$ collisions at $\sqrt{s} = 1.8$ TeV, Phys. Rev. D **62**, 072004 (2000).
[29] H1 Collaboration, Measurement of anti-deuteron photoproduction and a search for heavy stable charged particles at HERA, Eur. Phys. J. C **36**, 413 (2004).
[30] D. M. Asner *et al.* (CLEO Collaboration), Antideuteron production in $\Upsilon(nS)$ decays and the nearby continuum, Phys. Rev. D **75**, 012009 (2007).
[31] S. Schael *et al.* (ALEPH Collaboration), Deuteron and antideuteron production in e^+e^- collisions at the Z resonance, Phys. Lett. B **639**, 192 (2006).
[32] S. Acharya *et al.* (ALICE Collaboration), Production of deuterons, tritons, ^{3}He nuclei, and their antinuclei in pp collisions at $\sqrt{s} = 0.9$, 2.76, and 7 TeV, Phys. Rev. C **97**, 024615 (2018).
[33] S. Acharya *et al.* (ALICE Collaboration), Multiplicity dependence of light (anti-)nuclei production in p-Pb collisions at $\sqrt{s_{\rm NN}} = 5.02$ TeV, Phys. Lett. B **800**, 135043 (2020).
[34] S. Acharya *et al.* (ALICE Collaboration), Multiplicity dependence of (anti-)deuteron production in pp collisions at $\sqrt{s} = 7$ TeV, Phys. Lett. B **794**, 50 (2019).
[35] S. Acharya *et al.* (ALICE Collaboration), (Anti-)deuteron production in pp collisions at $\sqrt{s} = 13$ TeV, Eur. Phys. J. C **80**, 889 (2020).
[36] S. Acharya *et al.* (ALICE Collaboration), Jet-associated deuteron production in pp collisions at $\sqrt{s} = 13$ TeV, Phys. Lett. B **819**, 136440 (2021).
[37] S. Acharya *et al.* (ALICE Collaboration), Production of light (anti)nuclei in pp collisions at $\sqrt{s} = 13$ TeV, J. High Energy Phys. 01 (2022) 106.
[38] S. Acharya *et al.* (ALICE Collaboration), Production of light (anti)nuclei in pp collisions at $\sqrt{s} = 5.02$ TeV, Eur. Phys. J. C **82**, 289 (2022).
[39] J. I. Kapusta, Mechanisms for deuteron production in relativistic nuclear collisions, Phys. Rev. C **21**, 1301 (1980).
[40] S. Mrowczynski, Deuteron formation mechanism, J. Phys. G **13**, 1089 (1987).
[41] S. Mrowczynski, Anti-deuteron production and the size of the interaction zone, Phys. Lett. B **248**, 459 (1990).
[42] R. Scheibl and U. W. Heinz, Coalescence and flow in ultrarelativistic heavy ion collisions, Phys. Rev. C **59**, 1585 (1999).
[43] J. Steinheimer, K. Gudima, A. Botvina, I. Mishustin, M. Bleicher, and H. Stöcker, Hypernuclei, dibaryon and antinuclei production in high energy heavy ion collisions: Thermal production versus coalescence, Phys. Lett. B **714**, 85 (2012).
[44] F. Bellini and A. P. Kalweit, Testing production scenarios for (anti-)(hyper-)nuclei and exotica at energies available at the CERN Large Hadron Collider, Phys. Rev. C **99**, 054905 (2019).
[45] P. Braun-Munzinger, K. Redlich, and J. Stachel, Particle production in heavy ion collisions, in *Quark Gluon Plasma*, Vol. 3, edited by R. C. Hwa and X. N. Wang (World Scientific, Singapore, 2003).
[46] A. Andronic, P. Braun-Munzinger, J. Stachel, and H. Stocker, Production of light nuclei, hypernuclei and their antiparticles in relativistic nuclear collisions, Phys. Lett. B **697**, 203 (2011).
[47] J. Cleymans, S. Kabana, I. Kraus, H. Oeschler, K. Redlich, and N. Sharma, Antimatter production in proton-proton and heavy-ion collisions at ultrarelativistic energies, Phys. Rev. C **84**, 054916 (2011).
[48] A. Andronic, P. Braun-Munzinger, K. Redlich, and J. Stachel, Decoding the phase structure of QCD via particle production at high energy, Nature (London) **561**, 321 (2018).
[49] B. Dönigus, Light nuclei in the hadron resonance gas, Int. J. Mod. Phys. E **29**, 2040001 (2020).
[50] R. Hanbury Brown and R. Q. Twiss, A test of a new type of stellar interferometer on Sirius, Nature (London) **178**, 1046 (1956).
[51] R. Hanbury Brown and R. Q. Twiss, Correlation between photons in two coherent beams of light, Nature (London) **177**, 27 (1956).
[52] G. Goldhaber, S. Goldhaber, W.-Y. Lee, and A. Pais, Influence of Bose-Einstein statistics on the antiproton proton annihilation process, Phys. Rev. **120**, 300 (1960).
[53] J. Adam *et al.* (ALICE Collaboration), Two-pion femtoscopy in p-Pb collisions at $\sqrt{s_{\rm NN}} = 5.02$ TeV, Phys. Rev. C **91**, 034906 (2015).
[54] J. L. Nagle, B. S. Kumar, D. Kusnezov, H. Sorge, and R. Mattiello, Coalescence of deuterons in relativistic heavy ion collisions, Phys. Rev. C **53**, 367 (1996).
[55] K. Blum, R. Sato, and E. Waxman, Cosmic-ray antimatter, arXiv:1709.06507.
[56] K. Blum, Kenny Chun Yu Ng, R. Sato, and M. Takimoto, Cosmic rays, antihelium, and an old navy spotlight, Phys. Rev. D **96**, 103021 (2017).
[57] K.-J. Sun, C. M. Ko, and B. Dönigus, Suppression of light nuclei production in collisions of small systems at the Large Hadron Collider, Phys. Lett. B **792**, 132 (2019).
[58] V. Vovchenko, B. Dönigus, and H. Stoecker, Multiplicity dependence of light nuclei production at LHC energies in the canonical statistical model, Phys. Lett. B **785**, 171 (2018).
[59] V. Vovchenko, B. Dönigus, and H. Stoecker, Canonical statistical model analysis of p-p, p-Pb, and Pb-Pb collisions at energies available at the CERN Large Hadron Collider, Phys. Rev. C **100**, 054906 (2019).
[60] P. Castorina and H. Satz, Causality constraints on hadron production in high energy collisions, Int. J. Mod. Phys. E **23**, 1450019 (2014).
[61] S. Acharya *et al.* (ALICE Collaboration), Global baryon number conservation encoded in net-proton fluctuations measured in Pb-Pb collisions at $\sqrt{s_{\rm NN}} = 2.76$ TeV, Phys. Lett. B **807**, 135564 (2020).
[62] X. Xu and R. Rapp, Production of light nuclei at thermal freeze-out in heavy-ion collisions, Eur. Phys. J. A **55**, 68 (2019).
[63] V. Vovchenko, K. Gallmeister, J. Schaffner-Bielich, and C. Greiner, Nucleosynthesis in heavy-ion collisions at the LHC via the Saha equation, Phys. Lett. B **800**, 135131 (2020).
[64] T. Neidig, K. Gallmeister, C. Greiner, M. Bleicher, and V. Vovchenko, Towards solving the puzzle of high temperature light (anti)-nuclei production in ultra-relativistic heavy ion collisions, Phys. Lett. B **827**, 136891 (2022).
[65] S. Acharya *et al.* (ALICE Collaboration), Production of charged pions, kaons, and (anti-)protons in Pb-Pb and inelastic pp collisions at $\sqrt{s_{NN}} = 5.02$ TeV, Phys. Rev. C **101**, 044907 (2020).

[66] K. Aamodt *et al.* (ALICE Collaboration), The ALICE experiment at the CERN LHC, J. Instrum. **3**, S08002 (2008).
[67] ALICE Collaboration, Performance of the ALICE Experiment at the CERN LHC, Int. J. Mod. Phys. A **29**, 1430044 (2014).
[68] ALICE Collaboration, Alignment of the ALICE Inner Tracking System with cosmic-ray tracks, J. Instrum. **5**, P03003 (2010).
[69] J. Alme *et al.*, The ALICE TPC, a large 3-dimensional tracking device with fast readout for ultra-high multiplicity events, Nucl. Instrum. Methods Phys. Res., Sect. A **622**, 316 (2010).
[70] A. Akindinov *et al.*, Performance of the ALICE Time-Of-Flight detector at the LHC, Eur. Phys. J. Plus **128**, 44 (2013).
[71] S. Acharya *et al.* (ALICE Collaboration), The ALICE Transition Radiation Detector: construction, operation, and performance, Nucl. Instrum. Methods Phys. Res., Sect. A **881**, 88 (2018).
[72] ALICE Collaboration, Performance of the ALICE VZERO system, J. Instrum. **8**, P10016 (2013).
[73] W. Herr, Beam-beam interactions, CERN report (unpublished), https://cds.cern.ch/record/941319.
[74] X.-N. Wang and M. Gyulassy, HIJING: A Monte Carlo model for multiple jet production in *pp*, *pA* and *AA* collisions, Phys. Rev. D **44**, 3501 (1991).
[75] S. Agostinelli *et al.* (GEANT4 Collaboration), GEANT4: A simulation toolkit, Nucl. Instrum. Methods Phys. Res., Sect. A **506**, 250 (2003).
[76] S. Acharya *et al.* (ALICE Collaboration), Measurement of the Low-Energy Antideuteron Inelastic Cross Section, Phys. Rev. Lett. **125**, 162001 (2020).
[77] A. Auce, R. F. Carlson, A. J. Cox, A. Ingemarsson, R. Johansson, P. U. Renberg, O. Sundberg, and G. Tibell, Reaction cross sections for 38, 65, and 97 MeV deuterons on targets from ^{9}Be to ^{208}Pb, Phys. Rev. C **53**, 2919 (1996).
[78] F. G. Binon *et al.*, Absorption cross-sections of 25 GeV/c antideuterons in Li, C, Al, Cu and Pb, Phys. Lett. B **31**, 230 (1970).
[79] J. Jaros *et al.*, Nucleus-nucleus total cross sections for light nuclei at 1.55 and 2.89 GeV/*c* per nucleon, Phys. Rev. C **18**, 2273 (1978).
[80] S. P. Denisov, S. V. Donskov, Yu. P. Gorin, V. A. Kachanov, V. M. Kutjin, A. I. Petrukhin, Yu. D. Prokoshkin, E. A. Razuvaev, R. S. Shuvalov, and D. A. Stojanova, Measurements of anti-deuteron absorption and stripping cross sections at the momentum 13.3 GeV/c, Nucl. Phys. B **31**, 253 (1971).
[81] E. Schnedermann, J. Sollfrank, and U. W. Heinz, Thermal phenomenology of hadrons from 200*A* GeV S+S collisions, Phys. Rev. C **48**, 2462 (1993).
[82] F. Reif, *Fundamentals of Statistical and Thermal Physics* (McGraw-Hill, New York, 1965).
[83] P. Braun-Munzinger and B. Dönigus, Loosely-bound objects produced in nuclear collisions at the LHC, Nucl. Phys. A **987**, 144 (2019).
[84] J. Adam *et al.* (ALICE Collaboration), One-dimensional pion, kaon, and proton femtoscopy in Pb-Pb collisions at $\sqrt{s_{NN}} =$ 2.76 TeV, Phys. Rev. C **92**, 054908 (2015).
[85] S. Sombun, K. Tomuang, A. Limphirat, P. Hillmann, C. Herold, J. Steinheimer, Y. Yan, and M. Bleicher, Deuteron production from phase-space coalescence in the UrQMD approach, Phys. Rev. C **99**, 014901 (2019).
[86] T. Reichert, J. Steinheimer, V. Vovchenko, B. Dönigus, and M. Bleicher, Energy dependence of light hypernuclei production in heavy-ion collisions from a coalescence and statistical-thermal model perspective, Phys. Rev. C **107**, 014912 (2023).
[87] B. Dönigus, G. Röpke, and D. Blaschke, Deuteron yields from heavy-ion collisions at energies available at the CERN Large Hadron Collider: Continuum correlations and in-medium effects, Phys. Rev. C **106**, 044908 (2022).
[88] N. Sharma, L. Kumar, P. M. Lo, and K. Redlich, Light nuclei production in *pp* and *pA* collisions in the baryon canonical ensemble, Phys. Rev. C **107**, 054903 (2023).
[89] V. Vovchenko and V. Koch, Centrality dependence of proton and light nuclei yields as a consequence of baryon annihilation in the hadronic phase, Phys. Lett. B **835**, 137577 (2022).
[90] A. Dainese, M. Mangano, A. B. Meyer, A. Nisati, G. Salam, and M. A. Vesterinen, Report on the Physics at the HL-LHC, and Perspectives for the HE-LHC, CERN Technical Report No. CERN-2019-007, 2019 (unpublished), https://cds.cern.ch/record/2703572.

S. Acharya,[125] D. Adamová,[86] A. Adler,[69] G. Aglieri Rinella,[32] M. Agnello,[29] N. Agrawal,[50] Z. Ahammed,[132] S. Ahmad,[15] S. U. Ahn,[70] I. Ahuja,[37] A. Akindinov,[140] M. Al-Turany,[97] D. Aleksandrov,[140] B. Alessandro,[55] H. M. Alfanda,[6] R. Alfaro Molina,[66] B. Ali,[15] A. Alici,[25] N. Alizadehvandchali,[114] A. Alkin,[32] J. Alme,[20] G. Alocco,[51] T. Alt,[63] I. Altsybeev,[140] M. N. Anaam,[6] C. Andrei,[45] A. Andronic,[135] V. Anguelov,[94] F. Antinori,[53] P. Antonioli,[50] N. Apadula,[74] L. Aphecetche,[103] H. Appelshäuser,[63] C. Arata,[73] S. Arcelli,[25] M. Aresti,[51] R. Arnaldi,[55] J. G. M. C. A. Arneiro,[110] I. C. Arsene,[19] M. Arslandok,[137] A. Augustinus,[32] R. Averbeck,[97] M. D. Azmi,[15] A. Badalà,[52] J. Bae,[104] Y. W. Baek,[40] X. Bai,[118] R. Bailhache,[63] Y. Bailung,[47] A. Balbino,[29] A. Baldisseri,[128] B. Balis,[2] D. Banerjee,[4] Z. Banoo,[91] R. Barbera,[26] F. Barile,[31] L. Barioglio,[95] M. Barlou,[78] G. G. Barnaföldi,[136] L. S. Barnby,[85] V. Barret,[125] L. Barreto,[110] C. Bartels,[117] K. Barth,[32] E. Bartsch,[63] N. Bastid,[125] S. Basu,[75] G. Batigne,[103] D. Battistini,[95] B. Batyunya,[141] D. Bauri,[46] J. L. Bazo Alba,[101] I. G. Bearden,[83] C. Beattie,[137] P. Becht,[97] D. Behera,[47] I. Belikov,[127] A. D. C. Bell Hechavarria,[135] F. Bellini,[25] R. Bellwied,[114] S. Belokurova,[140] V. Belyaev,[140] G. Bencedi,[136] S. Beole,[24] A. Bercuci,[45] Y. Berdnikov,[140] A. Berdnikova,[94] L. Bergmann,[94] M. G. Besoiu,[62] L. Betev,[32] P. P. Bhaduri,[132] A. Bhasin,[91] M. A. Bhat,[4] B. Bhattacharjee,[41] L. Bianchi,[24] N. Bianchi,[48] J. Bielčík,[35] J. Bielčíková,[86] J. Biernat,[107] A. P. Bigot,[127] A. Bilandzic,[95] G. Biro,[136] S. Biswas,[4] N. Bize,[103] J. T. Blair,[108] D. Blau,[140] M. B. Blidaru,[97] N. Bluhme,[38] C. Blume,[63] G. Boca,[21,54] F. Bock,[87] T. Bodova,[20] A. Bogdanov,[140]

S. Boi,[22] J. Bok,[57] L. Boldizsár,[136] A. Bolozdynya,[140] M. Bombara,[37] P. M. Bond,[32] G. Bonomi,[131,54] H. Borel,[128] A. Borissov,[140] A. G. Borquez Carcamo,[94] H. Bossi,[137] E. Botta,[24] Y. E. M. Bouziani,[63] L. Bratrud,[63] P. Braun-Munzinger,[97] M. Bregant,[110] M. Broz,[35] G. E. Bruno,[96,31] M. D. Buckland,[23] D. Budnikov,[140] H. Buesching,[63] S. Bufalino,[29] O. Bugnon,[103] P. Buhler,[102] Z. Buthelezi,[67,121] S. A. Bysiak,[107] M. Cai,[6] H. Caines,[137] A. Caliva,[97] E. Calvo Villar,[101] J. M. M. Camacho,[109] P. Camerini,[23] F. D. M. Canedo,[110] M. Carabas,[124] A. A. Carballo,[32] F. Carnesecchi,[32] R. Caron,[126] L. A. D. Carvalho,[110] J. Castillo Castellanos,[128] F. Catalano,[24,29] C. Ceballos Sanchez,[141] I. Chakaberia,[74] P. Chakraborty,[46] S. Chandra,[132] S. Chapeland,[32] M. Chartier,[117] S. Chattopadhyay,[132] S. Chattopadhyay,[99] T. G. Chavez,[44] T. Cheng,[97,6] C. Cheshkov,[126] B. Cheynis,[126] V. Chibante Barroso,[32] D. D. Chinellato,[111] E. S. Chizzali,[95,*] J. Cho,[57] S. Cho,[57] P. Chochula,[32] P. Christakoglou,[84] C. H. Christensen,[83] P. Christiansen,[75] T. Chujo,[123] M. Ciacco,[29] C. Cicalo,[51] F. Cindolo,[50] M. R. Ciupek,[97] G. Clai,[50,†] F. Colamaria,[49] J. S. Colburn,[100] D. Colella,[96,31] M. Colocci,[32] M. Concas,[55,‡] G. Conesa Balbastre,[73] Z. Conesa del Valle,[72] G. Contin,[23] J. G. Contreras,[35] M. L. Coquet,[128] T. M. Cormier,[87,§] P. Cortese,[130,55] M. R. Cosentino,[112] F. Costa,[32] S. Costanza,[21,54] C. Cot,[72] J. Crkovská,[94] P. Crochet,[125] R. Cruz-Torres,[74] E. Cuautle,[64] P. Cui,[6] A. Dainese,[53] M. C. Danisch,[94] A. Danu,[62] P. Das,[80] P. Das,[4] S. Das,[4] A. R. Dash,[135] S. Dash,[46] A. De Caro,[28] G. de Cataldo,[49] J. de Cuveland,[38] A. De Falco,[22] D. De Gruttola,[28] N. De Marco,[55] C. De Martin,[23] S. De Pasquale,[28] S. Deb,[47] R. J. Debski,[2] K. R. Deja,[133] R. Del Grande,[95] L. Dello Stritto,[28] W. Deng,[6] P. Dhankher,[18] D. Di Bari,[31] A. Di Mauro,[32] R. A. Diaz,[141,7] T. Dietel,[113] Y. Ding,[126,6] R. Divià,[32] D. U. Dixit,[18] Ø. Djuvsland,[20] U. Dmitrieva,[140] A. Dobrin,[62] B. Dönigus,[63] J. M. Dubinski,[133] A. Dubla,[97] S. Dudi,[90] P. Dupieux,[125] M. Durkac,[106] N. Dzalaiova,[12] T. M. Eder,[135] R. J. Ehlers,[87] V. N. Eikeland,[20] F. Eisenhut,[63] D. Elia,[49] B. Erazmus,[103] F. Ercolessi,[25] F. Erhardt,[89] M. R. Ersdal,[20] B. Espagnon,[72] G. Eulisse,[32] D. Evans,[100] S. Evdokimov,[140] L. Fabbietti,[95] M. Faggin,[27] J. Faivre,[73] F. Fan,[6] W. Fan,[74] A. Fantoni,[48] M. Fasel,[87] P. Fecchio,[29] A. Feliciello,[55] G. Feofilov,[140] A. Fernández Téllez,[44] L. Ferrandi,[110] M. B. Ferrer,[32] A. Ferrero,[128] C. Ferrero,[55] A. Ferretti,[24] V. J. G. Feuillard,[94] V. Filova,[35] D. Finogeev,[140] F. M. Fionda,[51] F. Flor,[114] A. N. Flores,[108] S. Foertsch,[67] I. Fokin,[94] S. Fokin,[140] E. Fragiacomo,[56] E. Frajna,[136] U. Fuchs,[32] N. Funicello,[28] C. Furget,[73] A. Furs,[140] T. Fusayasu,[98] J. J. Gaardhøje,[83] M. Gagliardi,[24] A. M. Gago,[101] C. D. Galvan,[109] D. R. Gangadharan,[114] P. Ganoti,[78] C. Garabatos,[97] J. R. A. Garcia,[44] E. Garcia-Solis,[9] K. Garg,[103] C. Gargiulo,[32] K. Garner,[135] P. Gasik,[97] A. Gautam,[116] M. B. Gay Ducati,[65] M. Germain,[103] A. Ghimouz,[123] C. Ghosh,[132] M. Giacalone,[50,25] P. Giubellino,[97,55] P. Giubilato,[27] A. M. C. Glaenzer,[128] P. Glässel,[94] E. Glimos,[120] D. J. Q. Goh,[76] V. Gonzalez,[134] L. H. González-Trueba,[66] M. Gorgon,[2] S. Gotovac,[33] V. Grabski,[66] L. K. Graczykowski,[133] E. Grecka,[86] A. Grelli,[58] C. Grigoras,[32] V. Grigoriev,[140] S. Grigoryan,[141,1] F. Grosa,[32] J. F. Grosse-Oetringhaus,[32] R. Grosso,[97] D. Grund,[35] G. G. Guardiano,[111] R. Guernane,[73] M. Guilbaud,[103] K. Gulbrandsen,[83] T. Gundem,[63] T. Gunji,[122] W. Guo,[6] A. Gupta,[91] R. Gupta,[91] S. P. Guzman,[44] L. Gyulai,[136] M. K. Habib,[97] C. Hadjidakis,[72] F. U. Haider,[91] H. Hamagaki,[76] A. Hamdi,[74] M. Hamid,[6] Y. Han,[138] R. Hannigan,[108] M. R. Haque,[133] J. W. Harris,[137] A. Harton,[9] H. Hassan,[87] D. Hatzifotiadou,[50] P. Hauer,[42] L. B. Havener,[137] S. T. Heckel,[95] E. Hellbär,[97] H. Helstrup,[34] M. Hemmer,[63] T. Herman,[35] G. Herrera Corral,[8] F. Herrmann,[135] S. Herrmann,[126] K. F. Hetland,[34] B. Heybeck,[63] H. Hillemanns,[32] C. Hills,[117] B. Hippolyte,[127] F. W. Hoffmann,[69] B. Hofman,[58] B. Hohlweger,[84] G. H. Hong,[138] M. Horst,[95] A. Horzyk,[2] R. Hosokawa,[14] Y. Hou,[6] P. Hristov,[32] C. Hughes,[120] P. Huhn,[63] L. M. Huhta,[115] C. V. Hulse,[72] T. J. Humanic,[88] A. Hutson,[114] D. Hutter,[38] J. P. Iddon,[117] R. Ilkaev,[140] H. Ilyas,[13] M. Inaba,[123] G. M. Innocenti,[32] M. Ippolitov,[140] A. Isakov,[86] T. Isidori,[116] M. S. Islam,[99] M. Ivanov,[97] M. Ivanov,[12] V. Ivanov,[140] M. Jablonski,[2] B. Jacak,[74] N. Jacazio,[32] P. M. Jacobs,[74] S. Jadlovska,[106] J. Jadlovsky,[106] S. Jaelani,[82] L. Jaffe,[38] C. Jahnke,[111] M. J. Jakubowska,[133] M. A. Janik,[133] T. Janson,[69] M. Jercic,[89] S. Jia,[10] A. A. P. Jimenez,[64] F. Jonas,[87] J. M. Jowett,[32,97] J. Jung,[63] M. Jung,[63] A. Junique,[32] A. Jusko,[100] M. J. Kabus,[32,133] J. Kaewjai,[105] P. Kalinak,[59] A. S. Kalteyer,[97] A. Kalweit,[32] V. Kaplin,[140] A. Karasu Uysal,[71] D. Karatovic,[89] O. Karavichev,[140] T. Karavicheva,[140] P. Karczmarczyk,[133] E. Karpechev,[140] U. Kebschull,[69] R. Keidel,[139] D. L. D. Keijdener,[58] M. Keil,[32] B. Ketzer,[42] A. M. Khan,[6] S. Khan,[15] A. Khanzadeev,[140] Y. Kharlov,[140] A. Khatun,[116,15] A. Khuntia,[107] M. B. Kidson,[113] B. Kileng,[34] B. Kim,[16] C. Kim,[16] D. J. Kim,[115] E. J. Kim,[68] J. Kim,[138] J. S. Kim,[40] J. Kim,[68] M. Kim,[18,94] S. Kim,[17] T. Kim,[138] K. Kimura,[92] S. Kirsch,[63] I. Kisel,[38] S. Kiselev,[140] A. Kisiel,[133] J. P. Kitowski,[2] J. L. Klay,[5] J. Klein,[32] S. Klein,[74] C. Klein-Bösing,[135] M. Kleiner,[63] T. Klemenz,[95] A. Kluge,[32] A. G. Knospe,[114] C. Kobdaj,[105] T. Kollegger,[97] A. Kondratyev,[141] N. Kondratyeva,[140] E. Kondratyuk,[140] J. Konig,[63] S. A. Konigstorfer,[95] P. J. Konopka,[32] G. Kornakov,[133] S. D. Koryciak,[2] A. Kotliarov,[86] V. Kovalenko,[140] M. Kowalski,[107] V. Kozhuharov,[36] I. Králik,[59] A. Kravčáková,[37] L. Kreis,[97] M. Krivda,[100,59] F. Krizek,[86] K. Krizkova Gajdosova,[35] M. Kroesen,[94] M. Krüger,[63] D. M. Krupova,[35] E. Kryshen,[140] V. Kučera,[32] C. Kuhn,[127] P. G. Kuijer,[84] T. Kumaoka,[123] D. Kumar,[132] L. Kumar,[90] N. Kumar,[90] S. Kumar,[31] S. Kundu,[32] P. Kurashvili,[79] A. Kurepin,[140] A. B. Kurepin,[140] A. Kuryakin,[140] S. Kushpil,[86] J. Kvapil,[100] M. J. Kweon,[57] J. Y. Kwon,[57] Y. Kwon,[138] S. L. La Pointe,[38] P. La Rocca,[26] Y. S. Lai,[74] A. Lakrathok,[105] M. Lamanna,[32] R. Langoy,[119] P. Larionov,[32] E. Laudi,[32] L. Lautner,[32,95] R. Lavicka,[102] T. Lazareva,[140] R. Lea,[131,54] H. Lee,[104] G. Legras,[135] J. Lehrbach,[38]

R. C. Lemmon,[85] I. León Monzón,[109] M. M. Lesch,[95] E. D. Lesser,[18] M. Lettrich,[95] P. Lévai,[136] X. Li,[10] X. L. Li,[6] J. Lien,[119] R. Lietava,[100] I. Likmeta,[114] B. Lim,[24,16] S. H. Lim,[16] V. Lindenstruth,[38] A. Lindner,[45] C. Lippmann,[97] A. Liu,[18] D. H. Liu,[6] J. Liu,[117] I. M. Lofnes,[20] C. Loizides,[87] S. Lokos,[107] J. Lomker,[58] P. Loncar,[33] J. A. Lopez,[94] X. Lopez,[125] E. López Torres,[7] P. Lu,[97,118] J. R. Luhder,[135] M. Lunardon,[27] G. Luparello,[56] Y. G. Ma,[39] A. Maevskaya,[140] M. Mager,[32] T. Mahmoud,[42] A. Maire,[127] M. V. Makariev,[36] M. Malaev,[140] G. Malfattore,[25] N. M. Malik,[91] Q. W. Malik,[19] S. K. Malik,[91] L. Malinina,[141,‖] D. Mal'Kevich,[140] D. Mallick,[80] N. Mallick,[47] G. Mandaglio,[30,52] V. Manko,[140] F. Manso,[125] V. Manzari,[49] Y. Mao,[6] G. V. Margagliotti,[23] A. Margotti,[50] A. Marín,[97] C. Markert,[108] P. Martinengo,[32] J. L. Martinez,[114] M. I. Martínez,[44] G. Martínez García,[103] S. Masciocchi,[97] M. Masera,[24] A. Masoni,[51] L. Massacrier,[72] A. Mastroserio,[129,49] O. Matonoha,[75] P. F. T. Matuoka,[110] A. Matyja,[107] C. Mayer,[107] A. L. Mazuecos,[32] F. Mazzaschi,[24] M. Mazzilli,[32] J. E. Mdhluli,[121] A. F. Mechler,[63] Y. Melikyan,[43,140] A. Menchaca-Rocha,[66] E. Meninno,[102,28] A. S. Menon,[114] M. Meres,[12] S. Mhlanga,[113,67] Y. Miake,[123] L. Micheletti,[55] L. C. Migliorin,[126] D. L. Mihaylov,[95] K. Mikhaylov,[141,140] A. N. Mishra,[136] D. Miśkowiec,[97] A. Modak,[4] A. P. Mohanty,[58] B. Mohanty,[80] M. Mohisin Khan,[15,¶] M. A. Molander,[43] Z. Moravcova,[83] C. Mordasini,[95] D. A. Moreira De Godoy,[135] I. Morozov,[140] A. Morsch,[32] T. Mrnjavac,[32] V. Muccifora,[48] S. Muhuri,[132] J. D. Mulligan,[74] A. Mulliri,[22] M. G. Munhoz,[110] R. H. Munzer,[63] H. Murakami,[122] S. Murray,[113] L. Musa,[32] J. Musinsky,[59] J. W. Myrcha,[133] B. Naik,[121] A. I. Nambrath,[18] B. K. Nandi,[46] R. Nania,[50] E. Nappi,[49] A. F. Nassirpour,[75] A. Nath,[94] C. Nattrass,[120] M. N. Naydenov,[36] A. Neagu,[19] A. Negru,[124] L. Nellen,[64] S. V. Nesbo,[34] G. Neskovic,[38] D. Nesterov,[140] B. S. Nielsen,[83] E. G. Nielsen,[83] S. Nikolaev,[140] S. Nikulin,[140] V. Nikulin,[140] F. Noferini,[50] S. Noh,[11] P. Nomokonov,[141] J. Norman,[117] N. Novitzky,[123] P. Nowakowski,[133] A. Nyanin,[140] J. Nystrand,[20] M. Ogino,[76] A. Ohlson,[75] V. A. Okorokov,[140] J. Oleniacz,[133] A. C. Oliveira Da Silva,[120] M. H. Oliver,[137] A. Onnerstad,[115] C. Oppedisano,[55] A. Ortiz Velasquez,[64] J. Otwinowski,[107] M. Oya,[92] K. Oyama,[76] Y. Pachmayer,[94] S. Padhan,[46] D. Pagano,[131,54] G. Paić,[64] A. Palasciano,[49] S. Panebianco,[128] H. Park,[123] H. Park,[104] J. Park,[57] J. E. Parkkila,[32] R. N. Patra,[91] B. Paul,[22] H. Pei,[6] T. Peitzmann,[58] X. Peng,[6] M. Pennisi,[24] L. G. Pereira,[65] D. Peresunko,[140] G. M. Perez,[7] S. Perrin,[128] Y. Pestov,[140] V. Petráček,[35] V. Petrov,[140] M. Petrovici,[45] R. P. Pezzi,[103,65] S. Piano,[56] M. Pikna,[12] P. Pillot,[103] O. Pinazza,[50,32] L. Pinsky,[114] C. Pinto,[95] S. Pisano,[48] M. Płoskoń,[74] M. Planinic,[89] F. Pliquett,[63] M. G. Poghosyan,[87] B. Polichtchouk,[140] S. Politano,[29] N. Poljak,[89] A. Pop,[45] S. Porteboeuf-Houssais,[125] V. Pozdniakov,[141] K. K. Pradhan,[47] S. K. Prasad,[4] S. Prasad,[47] R. Preghenella,[50] F. Prino,[55] C. A. Pruneau,[134] I. Pshenichnov,[140] M. Puccio,[32] S. Pucillo,[24] Z. Pugelova,[106] S. Qiu,[84] L. Quaglia,[24] R. E. Quishpe,[114] S. Ragoni,[14,100] A. Rakotozafindrabe,[128] L. Ramello,[130,55] F. Rami,[127] S. A. R. Ramirez,[44] T. A. Rancien,[73] M. Rasa,[26] S. S. Räsänen,[43] R. Rath,[50] M. P. Rauch,[20] I. Ravasenga,[84] K. F. Read,[87,120] C. Reckziegel,[112] A. R. Redelbach,[38] K. Redlich,[79,**] C. A. Reetz,[97] A. Rehman,[20] F. Reidt,[32] H. A. Reme-Ness,[34] Z. Rescakova,[37] K. Reygers,[94] A. Riabov,[140] V. Riabov,[140] R. Ricci,[28] M. Richter,[19] A. A. Riedel,[95] W. Riegler,[32] C. Ristea,[62] M. Rodríguez Cahuantzi,[44] K. Røed,[19] R. Rogalev,[140] E. Rogochaya,[141] T. S. Rogoschinski,[63] D. Rohr,[32] D. Röhrich,[20] P. F. Rojas,[44] S. Rojas Torres,[35] P. S. Rokita,[133] G. Romanenko,[141] F. Ronchetti,[48] A. Rosano,[30,52] E. D. Rosas,[64] K. Roslon,[133] A. Rossi,[53] A. Roy,[47] S. Roy,[46] N. Rubini,[25] O. V. Rueda,[114,75] D. Ruggiano,[133] R. Rui,[23] B. Rumyantsev,[141] P. G. Russek,[2] R. Russo,[84] A. Rustamov,[81] E. Ryabinkin,[140] Y. Ryabov,[140] A. Rybicki,[107] H. Rytkonen,[115] W. Rzesa,[133] O. A. M. Saarimaki,[43] R. Sadek,[103] S. Sadhu,[31] S. Sadovsky,[140] J. Saetre,[20] K. Šafařík,[35] S. K. Saha,[4] S. Saha,[80] B. Sahoo,[46] R. Sahoo,[47] S. Sahoo,[60] D. Sahu,[47] P. K. Sahu,[60] J. Saini,[132] K. Sajdakova,[37] S. Sakai,[123] M. P. Salvan,[97] S. Sambyal,[91] I. Sanna,[32,95] T. B. Saramela,[110] D. Sarkar,[134] N. Sarkar,[132] P. Sarma,[41] V. Sarritzu,[22] V. M. Sarti,[95] M. H. P. Sas,[137] J. Schambach,[87] H. S. Scheid,[63] C. Schiaua,[45] R. Schicker,[94] A. Schmah,[94] C. Schmidt,[97] H. R. Schmidt,[93] M. O. Schmidt,[32] M. Schmidt,[93] N. V. Schmidt,[87] A. R. Schmier,[120] R. Schotter,[127] A. Schröter,[38] J. Schukraft,[32] K. Schwarz,[97] K. Schweda,[97] G. Scioli,[25] E. Scomparin,[55] J. E. Seger,[14] Y. Sekiguchi,[122] D. Sekihata,[122] I. Selyuzhenkov,[97,140] S. Senyukov,[127] J. J. Seo,[57] D. Serebryakov,[140] L. Šerkšnytė,[95] A. Sevcenco,[62] T. J. Shaba,[67] A. Shabetai,[103] R. Shahoyan,[32] A. Shangaraev,[140] A. Sharma,[90] B. Sharma,[91] D. Sharma,[46] H. Sharma,[107] M. Sharma,[91] N. Sharma,[90,††] S. Sharma,[76] S. Sharma,[91] U. Sharma,[91] A. Shatat,[72] O. Sheibani,[114] K. Shigaki,[92] M. Shimomura,[77] J. Shin,[11] S. Shirinkin,[140] Q. Shou,[39] Y. Sibiriak,[140] S. Siddhanta,[51] T. Siemiarczuk,[79] T. F. Silva,[110] D. Silvermyr,[75] T. Simantathammakul,[105] R. Simeonov,[36] B. Singh,[91] B. Singh,[95] R. Singh,[80] R. Singh,[91] R. Singh,[47] S. Singh,[15] V. K. Singh,[132] V. Singhal,[132] T. Sinha,[99] B. Sitar,[12] M. Sitta,[130,55] T. B. Skaali,[19] G. Skorodumovs,[94] M. Slupecki,[43] N. Smirnov,[137] R. J. M. Snellings,[58] E. H. Solheim,[19] J. Song,[114] A. Songmoolnak,[105] F. Soramel,[27] R. Spijkers,[84] I. Sputowska,[107] J. Staa,[75] J. Stachel,[94] I. Stan,[62] P. J. Steffanic,[120] S. F. Stiefelmaier,[94] D. Stocco,[103] I. Storehaug,[19] P. Stratmann,[135] S. Strazzi,[25] C. P. Stylianidis,[84] A. A. P. Suaide,[110] C. Suire,[72] M. Sukhanov,[140] M. Suljic,[32] R. Sultanov,[140] V. Sumberia,[91] S. Sumowidagdo,[82] S. Swain,[60] I. Szarka,[12] M. Szymkowski,[133] S. F. Taghavi,[95] G. Taillepied,[97] J. Takahashi,[111] G. J. Tambave,[20] S. Tang,[125,6] Z. Tang,[118] J. D. Tapia Takaki,[116] N. Tapus,[124] L. A. Tarasovicova,[135] M. G. Tarzila,[45] G. F. Tassielli,[31] A. Tauro,[32] G. Tejeda Muñoz,[44] A. Telesca,[32] L. Terlizzi,[24] C. Terrevoli,[114] G. Tersimonov,[3] S. Thakur,[4] D. Thomas,[108] A. Tikhonov,[140] A. R. Timmins,[114] M. Tkacik,[106] T. Tkacik,[106] A. Toia,[63] R. Tokumoto,[92] N. Topilskaya,[140]

M. Toppi,[48] F. Torales-Acosta,[18] T. Tork,[72] A. G. Torres Ramos,[31] A. Trifiró,[30,52] A. S. Triolo,[30,52] S. Tripathy,[50] T. Tripathy,[46] S. Trogolo,[32] V. Trubnikov,[3] W. H. Trzaska,[115] T. P. Trzcinski,[133] A. Tumkin,[140] R. Turrisi,[53] T. S. Tveter,[19] K. Ullaland,[20] B. Ulukutlu,[95] A. Uras,[126] M. Urioni,[54,131] G. L. Usai,[22] M. Vala,[37] N. Valle,[21] L. V. R. van Doremalen,[58] M. van Leeuwen,[84] C. A. van Veen,[94] R. J. G. van Weelden,[84] P. Vande Vyvre,[32] D. Varga,[136] Z. Varga,[136] M. Vasileiou,[78] A. Vasiliev,[140] O. Vázquez Doce,[48] V. Vechernin,[140] E. Vercellin,[24] S. Vergara Limón,[44] L. Vermunt,[97] R. Vértesi,[136] M. Verweij,[58] L. Vickovic,[33] Z. Vilakazi,[121] O. Villalobos Baillie,[100] A. Villani,[23] G. Vino,[49] A. Vinogradov,[140] T. Virgili,[28] V. Vislavicius,[75] A. Vodopyanov,[141] B. Volkel,[32] M. A. Völkl,[94] K. Voloshin,[140] S. A. Voloshin,[134] G. Volpe,[31] B. von Haller,[32] I. Vorobyev,[95] N. Vozniuk,[140] J. Vrláková,[37] C. Wang,[39] D. Wang,[39] Y. Wang,[39] A. Wegrzynek,[32] F. T. Weiglhofer,[38] S. C. Wenzel,[32] J. P. Wessels,[135] S. L. Weyhmiller,[137] J. Wiechula,[63] J. Wikne,[19] G. Wilk,[79] J. Wilkinson,[97] G. A. Willems,[135] B. Windelband,[94] M. Winn,[128] J. R. Wright,[108] W. Wu,[39] Y. Wu,[118] R. Xu,[6] A. Yadav,[42] A. K. Yadav,[132] S. Yalcin,[71] Y. Yamaguchi,[92] S. Yang,[20] S. Yano,[92] Z. Yin,[6] I.-K. Yoo,[16] J. H. Yoon,[57] S. Yuan,[20] A. Yuncu,[94] V. Zaccolo,[23] C. Zampolli,[32] F. Zanone,[94] N. Zardoshti,[32,100] A. Zarochentsev,[140] P. Závada,[61] N. Zaviyalov,[140] M. Zhalov,[140] B. Zhang,[6] L. Zhang,[39] S. Zhang,[39] X. Zhang,[6] Y. Zhang,[118] Z. Zhang,[6] M. Zhao,[10] V. Zherebchevskii,[140] Y. Zhi,[10] D. Zhou,[6] Y. Zhou,[83] J. Zhu,[97,6] Y. Zhu,[6] S. C. Zugravel,[55] and N. Zurlo[131,54]

(ALICE Collaboration)

[1]*A. I. Alikhanyan National Science Laboratory (Yerevan Physics Institute) Foundation, Yerevan, Armenia*
[2]*AGH University of Science and Technology, Cracow, Poland*
[3]*Bogolyubov Institute for Theoretical Physics, National Academy of Sciences of Ukraine, Kiev, Ukraine*
[4]*Department of Physics and Centre for Astroparticle Physics and Space Science (CAPSS), Bose Institute, Kolkata, India*
[5]*California Polytechnic State University, San Luis Obispo, California, USA*
[6]*Central China Normal University, Wuhan, China*
[7]*Centro de Aplicaciones Tecnológicas y Desarrollo Nuclear (CEADEN), Havana, Cuba*
[8]*Centro de Investigación y de Estudios Avanzados (CINVESTAV), Mexico City and Mérida, Mexico*
[9]*Chicago State University, Chicago, Illinois, USA*
[10]*China Institute of Atomic Energy, Beijing, China*
[11]*Chungbuk National University, Cheongju, Republic of Korea*
[12]*Faculty of Mathematics, Physics and Informatics, Comenius University Bratislava, Bratislava, Slovak Republic*
[13]*COMSATS University Islamabad, Islamabad, Pakistan*
[14]*Creighton University, Omaha, Nebraska, USA*
[15]*Department of Physics, Aligarh Muslim University, Aligarh, India*
[16]*Department of Physics, Pusan National University, Pusan, Republic of Korea*
[17]*Department of Physics, Sejong University, Seoul, Republic of Korea*
[18]*Department of Physics, University of California, Berkeley, California, USA*
[19]*Department of Physics, University of Oslo, Oslo, Norway*
[20]*Department of Physics and Technology, University of Bergen, Bergen, Norway*
[21]*Dipartimento di Fisica, Università di Pavia, Pavia, Italy*
[22]*Dipartimento di Fisica dell'Università and Sezione INFN, Cagliari, Italy*
[23]*Dipartimento di Fisica dell'Università and Sezione INFN, Trieste, Italy*
[24]*Dipartimento di Fisica dell'Università and Sezione INFN, Turin, Italy*
[25]*Dipartimento di Fisica e Astronomia dell'Università and Sezione INFN, Bologna, Italy*
[26]*Dipartimento di Fisica e Astronomia dell'Università and Sezione INFN, Catania, Italy*
[27]*Dipartimento di Fisica e Astronomia dell'Università and Sezione INFN, Padova, Italy*
[28]*Dipartimento di Fisica "E. R. Caianiello" dell'Università and Gruppo Collegato INFN, Salerno, Italy*
[29]*Dipartimento DISAT del Politecnico and Sezione INFN, Turin, Italy*
[30]*Dipartimento di Scienze MIFT, Università di Messina, Messina, Italy*
[31]*Dipartimento Interateneo di Fisica "M. Merlin" and Sezione INFN, Bari, Italy*
[32]*European Organization for Nuclear Research (CERN), Geneva, Switzerland*
[33]*Faculty of Electrical Engineering, Mechanical Engineering and Naval Architecture, University of Split, Split, Croatia*
[34]*Faculty of Engineering and Science, Western Norway University of Applied Sciences, Bergen, Norway*
[35]*Faculty of Nuclear Sciences and Physical Engineering, Czech Technical University in Prague, Prague, Czech Republic*
[36]*Faculty of Physics, Sofia University, Sofia, Bulgaria*
[37]*Faculty of Science, P. J. Šafárik University, Košice, Slovak Republic*
[38]*Frankfurt Institute for Advanced Studies, Johann Wolfgang Goethe-Universität Frankfurt, Frankfurt, Germany*
[39]*Fudan University, Shanghai, China*
[40]*Gangneung-Wonju National University, Gangneung, Republic of Korea*

[41]*Department of Physics, Gauhati University, Guwahati, India*
[42]*Helmholtz-Institut für Strahlen- und Kernphysik, Rheinische Friedrich-Wilhelms-Universität Bonn, Bonn, Germany*
[43]*Helsinki Institute of Physics (HIP), Helsinki, Finland*
[44]*High Energy Physics Group, Universidad Autónoma de Puebla, Puebla, Mexico*
[45]*Horia Hulubei National Institute of Physics and Nuclear Engineering, Bucharest, Romania*
[46]*Indian Institute of Technology Bombay (IIT), Mumbai, India*
[47]*Indian Institute of Technology Indore, Indore, India*
[48]*INFN, Laboratori Nazionali di Frascati, Frascati, Italy*
[49]*INFN, Sezione di Bari, Bari, Italy*
[50]*INFN, Sezione di Bologna, Bologna, Italy*
[51]*INFN, Sezione di Cagliari, Cagliari, Italy*
[52]*INFN, Sezione di Catania, Catania, Italy*
[53]*INFN, Sezione di Padova, Padova, Italy*
[54]*INFN, Sezione di Pavia, Pavia, Italy*
[55]*INFN, Sezione di Torino, Turin, Italy*
[56]*INFN, Sezione di Trieste, Trieste, Italy*
[57]*Inha University, Incheon, Republic of Korea*
[58]*Institute for Gravitational and Subatomic Physics (GRASP), Utrecht University/Nikhef, Utrecht, Netherlands*
[59]*Institute of Experimental Physics, Slovak Academy of Sciences, Košice, Slovak Republic*
[60]*Institute of Physics, Homi Bhabha National Institute, Bhubaneswar, India*
[61]*Institute of Physics of the Czech Academy of Sciences, Prague, Czech Republic*
[62]*Institute of Space Science (ISS), Bucharest, Romania*
[63]*Institut für Kernphysik, Johann Wolfgang Goethe-Universität Frankfurt, Frankfurt, Germany*
[64]*Instituto de Ciencias Nucleares, Universidad Nacional Autónoma de México, Mexico City, Mexico*
[65]*Instituto de Física, Universidade Federal do Rio Grande do Sul (UFRGS), Porto Alegre, Brazil*
[66]*Instituto de Física, Universidad Nacional Autónoma de México, Mexico City, Mexico*
[67]*iThemba LABS, National Research Foundation, Somerset West, South Africa*
[68]*Jeonbuk National University, Jeonju, Republic of Korea*
[69]*Fachbereich Informatik und Mathematik, Johann-Wolfgang-Goethe Universität Frankfurt Institut für Informatik, Frankfurt, Germany*
[70]*Korea Institute of Science and Technology Information, Daejeon, Republic of Korea*
[71]*KTO Karatay University, Konya, Turkey*
[72]*Laboratoire de Physique des 2 Infinis, Irène Joliot-Curie, Orsay, France*
[73]*Laboratoire de Physique Subatomique et de Cosmologie, Université Grenoble-Alpes, CNRS-IN2P3, Grenoble, France*
[74]*Lawrence Berkeley National Laboratory, Berkeley, California, USA*
[75]*Division of Particle Physics, Department of Physics, Lund University, Lund, Sweden*
[76]*Nagasaki Institute of Applied Science, Nagasaki, Japan*
[77]*Nara Women's University (NWU), Nara, Japan*
[78]*Department of Physics, School of Science, National and Kapodistrian University of Athens, Athens, Greece*
[79]*National Centre for Nuclear Research, Warsaw, Poland*
[80]*National Institute of Science Education and Research, Homi Bhabha National Institute, Jatni, India*
[81]*National Nuclear Research Center, Baku, Azerbaijan*
[82]*National Research and Innovation Agency - BRIN, Jakarta, Indonesia*
[83]*Niels Bohr Institute, University of Copenhagen, Copenhagen, Denmark*
[84]*Nikhef, National Institute for Subatomic Physics, Amsterdam, Netherlands*
[85]*Nuclear Physics Group, STFC Daresbury Laboratory, Daresbury, United Kingdom*
[86]*Nuclear Physics Institute of the Czech Academy of Sciences, Husinec-Řež, Czech Republic*
[87]*Oak Ridge National Laboratory, Oak Ridge, Tennessee, USA*
[88]*Ohio State University, Columbus, Ohio, USA*
[89]*Physics Department, Faculty of science, University of Zagreb, Zagreb, Croatia*
[90]*Physics Department, Panjab University, Chandigarh, India*
[91]*Physics Department, University of Jammu, Jammu, India*
[92]*Physics Program and International Institute for Sustainability with Knotted Chiral Meta Matter (SKCM2), Hiroshima University, Hiroshima, Japan*
[93]*Physikalisches Institut, Eberhard-Karls-Universität Tübingen, Tübingen, Germany*
[94]*Physikalisches Institut, Ruprecht-Karls-Universität Heidelberg, Heidelberg, Germany*
[95]*Physik Department, Technische Universität München, Munich, Germany*
[96]*Politecnico di Bari and Sezione INFN, Bari, Italy*
[97]*Research Division and ExtreMe Matter Institute EMMI, GSI Helmholtzzentrum für Schwerionenforschung GmbH, Darmstadt, Germany*
[98]*Saga University, Saga, Japan*

[99] *Saha Institute of Nuclear Physics, Homi Bhabha National Institute, Kolkata, India*
[100] *School of Physics and Astronomy, University of Birmingham, Birmingham, United Kingdom*
[101] *Sección Física, Departamento de Ciencias, Pontificia Universidad Católica del Perú, Lima, Peru*
[102] *Stefan Meyer Institut für Subatomare Physik (SMI), Vienna, Austria*
[103] *SUBATECH, IMT Atlantique, Nantes Université, CNRS-IN2P3, Nantes, France*
[104] *Sungkyunkwan University, Suwon City, Republic of Korea*
[105] *Suranaree University of Technology, Nakhon Ratchasima, Thailand*
[106] *Technical University of Košice, Košice, Slovak Republic*
[107] *The Henryk Niewodniczanski Institute of Nuclear Physics, Polish Academy of Sciences, Cracow, Poland*
[108] *The University of Texas at Austin, Austin, Texas, USA*
[109] *Universidad Autónoma de Sinaloa, Culiacán, Mexico*
[110] *Universidade de São Paulo (USP), São Paulo, Brazil*
[111] *Universidade Estadual de Campinas (UNICAMP), Campinas, Brazil*
[112] *Universidade Federal do ABC, Santo Andre, Brazil*
[113] *University of Cape Town, Cape Town, South Africa*
[114] *University of Houston, Houston, Texas, USA*
[115] *University of Jyväskylä, Jyväskylä, Finland*
[116] *University of Kansas, Lawrence, Kansas, USA*
[117] *University of Liverpool, Liverpool, United Kingdom*
[118] *University of Science and Technology of China, Hefei, China*
[119] *University of South-Eastern Norway, Kongsberg, Norway*
[120] *University of Tennessee, Knoxville, Tennessee, USA*
[121] *University of the Witwatersrand, Johannesburg, South Africa*
[122] *University of Tokyo, Tokyo, Japan*
[123] *University of Tsukuba, Tsukuba, Japan*
[124] *University Politehnica of Bucharest, Bucharest, Romania*
[125] *Université Clermont Auvergne, CNRS/IN2P3, LPC, Clermont-Ferrand, France*
[126] *Université de Lyon, CNRS/IN2P3, Institut de Physique des 2 Infinis de Lyon, Lyon, France*
[127] *Université de Strasbourg, CNRS, IPHC UMR 7178, F-67000 Strasbourg, France, Strasbourg, France*
[128] *Départment de Physique Nucléaire (DPhN), IRFU, Université Paris-Saclay Centre d'Etudes de Saclay (CEA), Saclay, France*
[129] *Università degli Studi di Foggia, Foggia, Italy*
[130] *Università del Piemonte Orientale, Vercelli, Italy*
[131] *Università di Brescia, Brescia, Italy*
[132] *Variable Energy Cyclotron Centre, Homi Bhabha National Institute, Kolkata, India*
[133] *Warsaw University of Technology, Warsaw, Poland*
[134] *Wayne State University, Detroit, Michigan, USA*
[135] *Westfälische Wilhelms-Universität Münster, Institut für Kernphysik, Münster, Germany*
[136] *Wigner Research Centre for Physics, Budapest, Hungary*
[137] *Yale University, New Haven, Connecticut, USA*
[138] *Yonsei University, Seoul, Republic of Korea*
[139] *Zentrum für Technologie und Transfer (ZTT), Worms, Germany*
[140] *Affiliated with an institute covered by a cooperation agreement with CERN*
[141] *Affiliated with an international laboratory covered by a cooperation agreement with CERN*

[*] Also at Max-Planck-Institut für Physik, Munich, Germany.
[†] Also at Italian National Agency for New Technologies, Energy and Sustainable Economic Development (ENEA), Bologna, Italy.
[‡] Also at Dipartimento DET del Politecnico di Torino, Turin, Italy.
[§] Deceased
[‖] Also at An institution covered by a cooperation agreement with CERN.
[¶] Also at Department of Applied Physics, Aligarh Muslim University, Aligarh, India.
[**] Also at Institute of Theoretical Physics, University of Wroclaw, Poland.
[††] Also at Indian Institute of Science Education and Research (IISER) Berhampur, Odisha, India.